

Received 17 August 2023, accepted 8 September 2023, date of publication 11 September 2023,  
date of current version 25 September 2023.

Digital Object Identifier 10.1109/ACCESS.2023.3314330

TOPICAL REVIEW

# AC Optimal Power Flow in Power Systems With Renewable Energy Integration: A Review of Formulations and Case Studies

ZONGJIE WANG<sup>1</sup>, (Member, IEEE), ABDOLLAH YOUNESI<sup>1</sup>, (Member, IEEE),  
M. VIVIENNE LIU<sup>2</sup>, (Student Member, IEEE), GE CLAIRE GUO<sup>3</sup>, (Member, IEEE),  
AND C. LINDSAY ANDERSON<sup>2</sup>, (Senior Member, IEEE)

<sup>1</sup>Department of Electrical and Computer Engineering, University of Connecticut, Storrs, CT 06268, USA

<sup>2</sup>Department of Systems Engineering, Cornell University, Ithaca, NY 14850, USA

<sup>3</sup>Department of Information Systems and Decision Science, University of Baltimore, Baltimore, MD 21202, USA

Corresponding author: Zongjie Wang (zongjie.wang@uconn.edu)

**ABSTRACT** The primary goal of a power system is to provide consumers with reliable access to power at the most economical cost. Under the declining costs of renewable energy sources, the increasing cost of natural gas, and growing emissions control policies, investment in variable renewable energy (VRE) sources including wind and solar is accelerating. As a fundamental optimization tool in the operation and planning of electric power systems, the optimal power flow (OPF) is critical for setting the optimal state of control variables by minimizing desired objective while satisfying all related constraints. However, a comprehensive review of the generic OPF framework that includes all categories of objectives, control variables, and constraints will provide a valuable background to many of the integration studies that are necessary to facilitate the transition of energy systems. A comprehensive OPF framework is essential for researchers to identify the most critical challenges to their applications to develop new solution methods to improve computational efficiency and to take advantage of the increasing computing power to reduce the number of approximations in OPF models. In this work, we aim to provide a comprehensive survey and a generic OPF formulation, along with a detailed explanation of the major formulations for conventional OPF objective functions, control variables, and network constraints, in particular those related to the handling of VREs. This article also highlights the modeling and challenges in the distribution system, and potential formulations to incorporate with the significant variability and intermittency of VRE sources. In addition to a discussion of various formulations and foci for the OPF problem, we compare the implications of these decisions on a small case study to highlight differences.

**INDEX TERMS** Control variables, equality constraints, inequality constraints, objective function, optimal power flow, renewable energy integration, traditional power systems.

## I. INTRODUCTION

Optimal power flow (OPF) decisions and plays a crucial role in the operation and planning of power systems. Formulations and solution methods of the OPF have a rich history in the literature, and are rapidly evolving with developments in the field of optimization. In general, OPF problems pursue

The associate editor coordinating the review of this manuscript and approving it for publication was Ehab Elsayed Elattar<sup>1</sup>.

the lowest cost operation of a power system, subject to power balance equations and other system constraints. The first OPF problem was introduced in 1962, when Carpentier extended the economic dispatch problem to include electric power flow equations to the model [1]. Prior to [1], the OPF decision had been made based on experience, judgment, rules of thumb, and heuristics [2].

To better understand the nature of OPF, it is necessary to introduce the three well-researched and closely related

problems in power systems literature: power flow, economic dispatch (ED), unit commitment (UC), as a precursor to the OPF. The power flow problem, also known as load flow, is fundamentally a network analysis problem. Power flow uses the generation, load, and transmission network equations to find voltage magnitudes and angles for a given network configuration. From the voltage and angle information states, the real and reactive generation, and load levels at all buses, as well as the real and reactive flows across all circuits, can be calculated. The second type of problem, the economic dispatch, is an optimization problem to allocate the system load among generating units in such a way that the total generation cost is minimized. The power losses in transmission lines are ignored and the power flow limitations are not considered in the economic dispatch problem. The unit commitment and economic dispatch problem has been solved in a two-stage context where the day-ahead unit commitment problem is solved in the first stage to determine the hourly commitment status for each generating unit, and the economic dispatch problem is solved in the second stage in real time to dispatch the committed resources to supply the load in the system. The last type of problem, the OPF, seeks the optimal operation of electric power generation, transmission, and sometimes distribution networks subject to the power flow and other operational constraints such as load balance, generator upper and lower limits, transmission stability and voltage constraints. Sometimes OPF is also referred to as security-constrained economic dispatch. The key differences in unit commitment, ED, power flow, and OPF are presented in Fig. 1.

According to Fig. 1, AC OPF, taking into account all system constraints is the most effective method for real-power systems' planning and operation. In this section, the IEEE 14-bus test case is employed with GAMS software to calculate the ED, DC OPF, and AC OPF under different system constraints that are added in the formulation. The simulation results are shown in Table 1.

In ED formulation, only the max/min output of power plants is considered and other constraints are ignored. Therefore, ED has dispatched the demand among the cheapest generation units, regardless of the location of the units. Table 1 shows that by considering the line limits along with generation unit max/min output level, the generation cost of DC OPF formulation has increased under congestion of transmission lines.

The demand is dispatched among generation units under the consideration of generation cost and line limits. It is evident that under the transmission line congestion, not all load is supplied (i.e. load loss in Table 1). Furthermore, Table 1 shows that by considering the reactive power dispatch and voltage inequality constraints, the dispatch of the demand among the generation units is significantly different. In the AC OPF formulation, the generation cost has increased due to the inclusion of line limits, and the need to maintain bus voltages within desirable limits. As a result, the AC OPF can be considered as a comprehensive and practical power

**TABLE 1. The impacts of power system constraints on the system planning through economic dispatch (ED), DC optimal power flow (DC OPF), and AC optimal power flow (AC OPF) in IEEE 14-bus test case.**

Bus no.	ED			DC OPF			AC OPF with 10% voltage dev.			AC OPF with 5% voltage dev.		
	$P_g$	$Q_g$	$V_i$	$P_g$	$Q_g$	$V_i$	$P_g$	$Q_g$	$V_i$	$P_g$	$Q_g$	$V_i$
1	305.4302	-	-	284.82	-	1	70.71	0	1	0	0	1
2	52.5698	-	-	11.06	-	1	140	19.91	0.9985	123.46	-18.12	1.0010
3	0	-	-	10.17	-	1	100	40.00	1.0006	100	40	1.0190
4	-	-	-	-	-	1	-	-	0.9532	-	-	0.9875
5	-	-	-	-	-	1	-	-	0.9576	-	-	0.9896
6	0	-	-	23.59	-	1	14.38	24.00	0.9434	67.72	24.00	0.9918
7	-	-	-	-	-	1	-	-	0.9394	-	-	0.9875
8	0	-	-	18.00	-	1	18.00	17.11	0.9687	50.49	21.16	1.0239
9	-	-	-	-	-	1	-	-	0.9189	-	-	0.9655
10	-	-	-	-	-	1	-	-	0.99149	-	-	0.9618
11	-	-	-	-	-	1	-	-	0.9251	-	-	0.9726
12	-	-	-	-	-	1	-	-	0.9458	-	-	0.9771
13	-	-	-	-	-	1	-	-	0.9231	-	-	0.9753
14	-	-	-	-	-	1	-	-	0.9000	-	-	0.9500
Load loss	0			10.3641			14.9106			16.3287		
Generation Cost (\$)	7207.0499			8023.2098			9561.6215			11237.3815		
Simulation time (s)	0.07			0.092			0.155			0.177		
Iteration	5			12			32			35		

system scheduling tool and is able to provide more accurate solutions than ED and DC OPF for power system planning and operation.

A review of the literature on various aspects of economic dispatch with emphasis on OPF during the time period of 1977-1988 is provided in [3]. Based on different optimization methods, paper [4] surveyed over three hundred articles and summarized the evolution of OPF publications through 1991. Momoh et al. reviewed the OPF literature over 1962-1993, focusing on the application of nonlinear and quadratic programming and Newton-based, linear programming and interior point methods in [5] and [6]. Zhang and Tolbert surveyed the OPF formulations and summarized the OPF solution methods into nine categories [7], [8]. To cope with the deregulation of power market and more complex OPF problems, papers [9], [10] surveyed the optimization algorithms for OPF with a focus on recent methods that emerged to deal with highly complex OPF models. Paper [11] reviewed different formulations and solution methods of the optimal power dynamic dispatch problem. Frank et al. provided a comprehensive survey and comparison of OPF optimization algorithms, in [12] reviewed the deterministic solution methods and in [13] examined the stochastic and hybrid approaches. In [2], the authors reviewed the evolution of OPF in the literature and provided a summary of major formulations of OPF. Paper [14] addressed the challenges with the traditional methods in OPF problems and

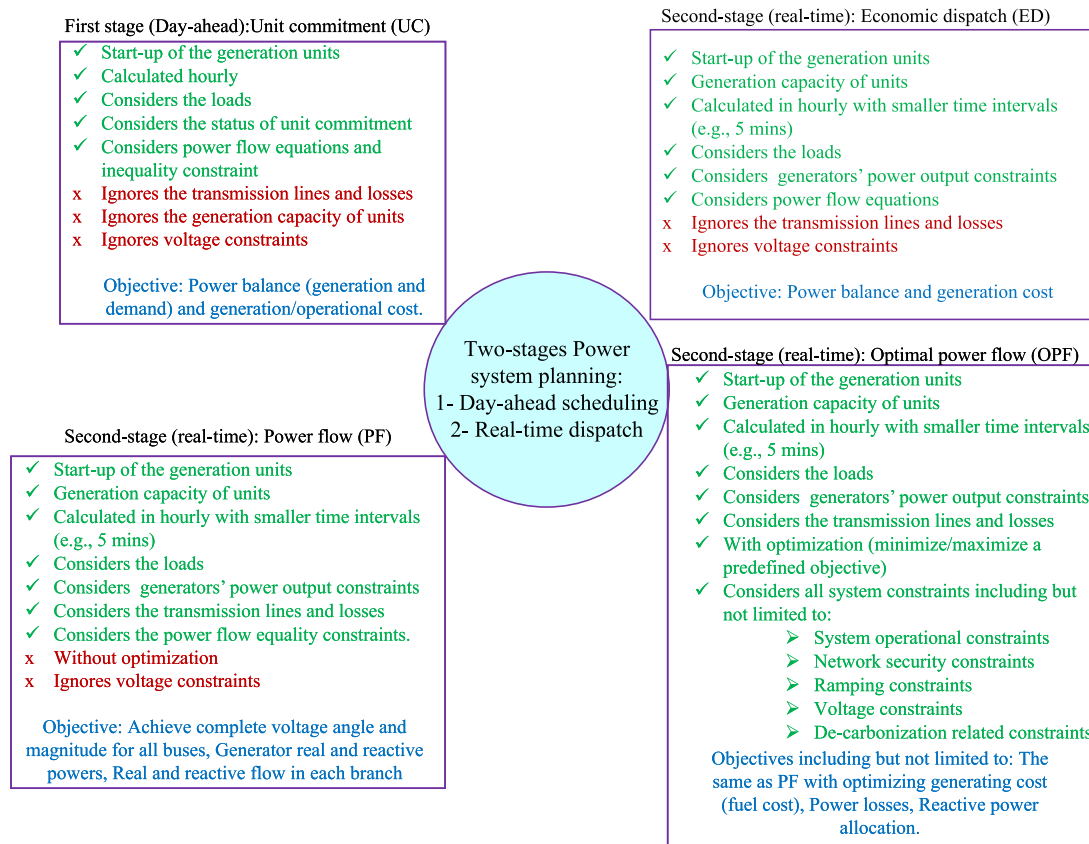


**FIGURE 1.** The overarching schematic of the two-stage power system planning including day-ahead scheduling and real-time dispatch.

reviewed the recent optimization techniques. In [15], Frank and Rebennack provided an introduction to OPF modeling from an operations research perspective with emphasis on electrical engineering theory and mechanics of the OPF formulation. In [16] compared different OPF approaches in distribution networks with corresponding objective functions and constraints. Reference [17] offered a critical review of the major advancements in real-time OPF solution approaches. Paper [18] reviewed the success of conic optimization for power system applications.

Despite the sheer volume of literature addressing OPF, the existing review articles on this topic focus heavily on optimization techniques and solution algorithms. Few surveys have included the major formulations of OPF and thus lacked a complete survey and explanations of the variables, objectives, and constraints. However, a generic OPF formulation is essential for the operations researcher to identify the challenges to solving OPF problems, to develop new solution methods to improve computational efficiency, and to take advantage of the increasing computing power to reduce the number of approximations in OPF models. For example, advances in mixed-integer programming (MIP) has achieved significant speed improvement and is replacing other optimization methods in ISO markets [2], saving

American electricity market participants over one-half billion dollars per year [19]. The goal of this survey is to provide a generic formulation of OPF, including a complete summary of objective functions, control variables and network constraints.

Another issue with the existing surveys is that the OPF models are restricted to conventional power generation that use depletable resources. The declining price of renewable energy technologies and the implementation of emissions control policies will lead to a system dominated by VRE sources in the future. To this end, this article aims to provide a complete and detailed survey of OPF formulations with VREs. By presenting a summary of OPF formulations with VRE integration, this survey also highlights the key modeling and computational challenges, along with potential formulations to incorporate with the significant variability and intermittency of VREs.

Another investigation followed in this paper is to numerically evaluate the impact of various objective functions on the OPF results. For this aim, the IEEE RTS test case is considered and multi-period OPF is performed by using GAMS. The simulation results and impacts of each objective function on the power system performance are illustrated and discussed.

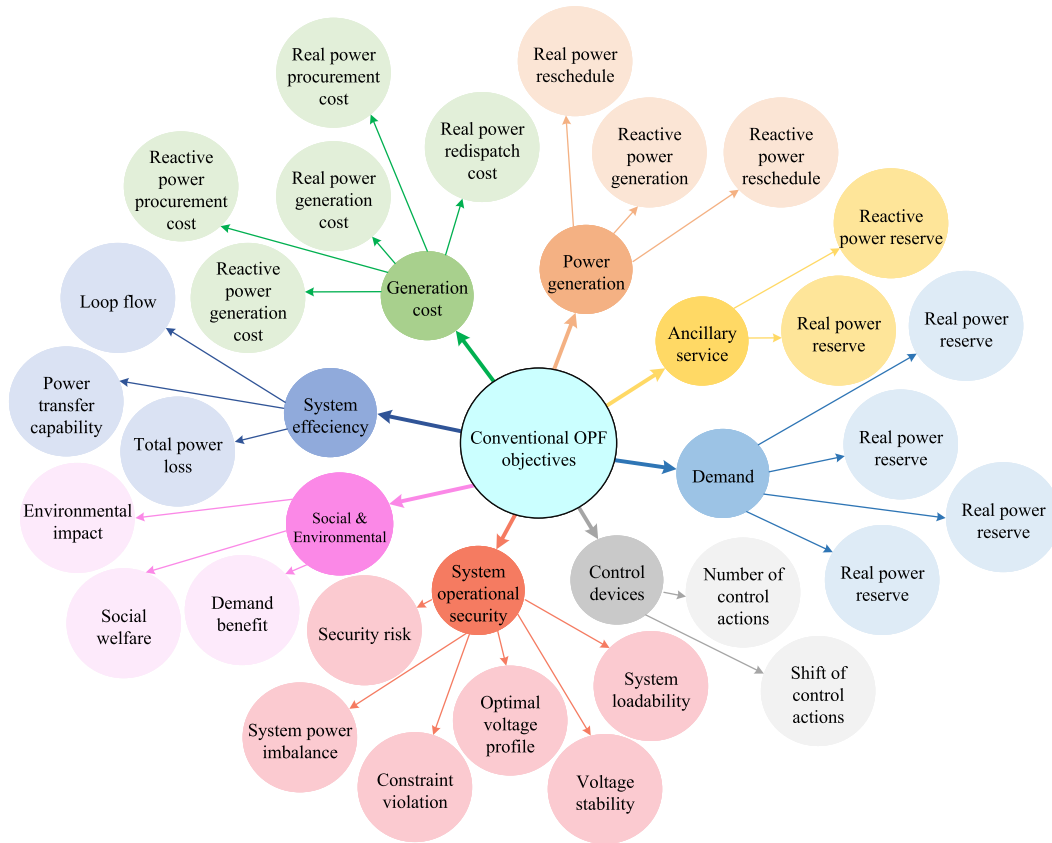


FIGURE 2. Categorization of conventional OPF objectives.

The remainder of this article is organized as follows. Section II presents a brief introduction to the basic mathematical formulation of OPF problems. Section III describes the generic OPF formulation with conventional electricity generators and provides a complete summary of objective functions, control variables and network constraints with detailed explanations and numerical evaluations. The OPF formulation with VRE integration is provided in Section IV. OPF in distribution systems with DERs is briefly discussed in Section V. Promising areas of future work are concluded and summarized in Section VI.

## II. BASIC OPF PROBLEM MODELLING

OPF problem formulation is concerned with the setting of control variables for the steady-state performance of the power system with respect to a predefined objective function, subject to various equality and inequality network constraints.

The majority of OPF formulations can be represented using the following general form:

$$\begin{aligned} &\min f(u, x) \\ &s.t. \quad g(u, x) = 0 \\ &\quad \quad h(u, x) \leq 0 \end{aligned} \quad (1)$$

In this formulation,  $x$  represents state variables and  $u$  represents control variables. The objective function  $f(u, x)$  represents the system optimization goal. Vector functions  $g(u, x)$  and  $h(u, x)$  represent system equality and inequality constraints, respectively. Depending on the selection of  $f$ ,  $g$  and  $h$ , the OPF problem may become a nonlinear, convex, linear or mixed integer-linear/nonlinear problem.

## III. SURVEY OF CONVENTIONAL OPF FORMULATIONS

Literature related to both conventional OPF problems and OPF considering renewable integration are surveyed. In this section, a survey of conventional OPF objective, control variables and constraints is conducted. Summary tables and categorization graphs are provided, along with highlights of each formulation.

### A. CONVENTIONAL OBJECTIVE FUNCTIONS

Fig. 2 shows a categorization of the conventional objectives found in the literature. Table 2 provides the list of references with formulations based on each of these objective categories.

Within the category of cost related objectives, some are represented in a linear function, such as the reserve cost objectives formulated as a linear function of reserves [42], [60], [61], procurement cost calculated from a linear function

TABLE 2. Conventional OPF objectives with references.

Generation Cost Related	
Objective	References
Real power generation cost	[20]–[49]
Real power re-dispatch cost	[45], [48], [50]–[54]
Real power procurement cost	[55]
Reactive power generation cost	[49], [56]
Reactive power procurement cost	[57]
Power Generation Related	
Objective	References
Real power reschedule	[58], [59]
Reactive power generation	[57]
Reactive power reschedule	[58]
Ancillary Service Related	
Objective	References
Real power reserve cost	[31], [33], [42]
Reactive power reserve (cost)	[45], [48], [57], [60], [61]
Demand Related	
Objective	References
Load shedding amount	[50], [58], [59], [62], [63]
Load shedding cost	[22], [32], [33], [53], [54]
Load shedding benefit	[64]
Supplied load	[65]
Control Devices Related	
Objective	References
Number/cost of control actions	[37], [66], [67]
Shift of control actions	[40], [58], [68]
System Operational Security Related	
Objective	References
System loadability	[26]
Voltage stability	[35], [44], [57]
Constraint violation	[32], [67], [69]
System power imbalance	[42]
Security risk	[70]
System Efficiency Related	
Objective	References
Power losses	[13], [21], [27], [29], [35], [37], [43], [52], [57], [63], [66], [71], [72]
Power transfer capability	[28], [29], [62], [73]–[80]
Loop flow	[68]
Social Environmental Related	
Objective	References
Demand benefit	[81]
Social welfare	[30], [53], [70], [75], [82]–[88]
Environmental impact	[29], [35]

of purchased amount [55], [57], re-dispatch cost written in a linear function of dispatch [52], [53], [54], and security risk represented by a linear function of interruption costs of loads [70]. The generation cost [40], [41], [42], [43], [44], [45], [46], [47], load shedding cost [32], control costs [58], and emission functions [29], [35], on the other hand, are primarily represented with a quadratic form. The minimization of the power generation cost is the objective commonly adopted in the existing literature [21], [29], [32], [33], [34], [35], [36], [37], [38], [40], [41], [42], [43], [44], [45], [46], [47], [49]. Although several studies use a linear cost function to approximate the real power generation cost [36], [38], most of the current research employed a second order polynomial function to compute the total cost for the real power generation cost and reactive power generation cost [21], [29], [32], [33], [34], [35], [36], [37], [38], [40], [41], [42], [43], [44], [45], [46], [47], [49]. In addition to adopting the quadratic functions to represent the real power generation cost, some scholars also consider the valve-point effects to obtain a more accurate model and modify the quadratic function to a non-smooth cost function to include the ripple curve created by valve-point effect [29], [32], [34]. Mathematical formulas and explanations under each specific conventional objective function are shown in details as follows.

### 1) REAL POWER GENERATION COST

Minimization of active power generation cost or generation fuel cost is the most common optimization objective for the economic-based operation of the power system.

### a: QUADRATIC FORM

$$f_1(P_G) = \sum_{i=1}^{N_G} (a_i + b_i P_{Gi} + c_i P_{Gi}^2) \quad (2)$$

where

- $N_G$  is the number of generators including the slack generators in the power systems under study;
- $a_i$ ,  $b_i$ ,  $c_i$  are the basic, linear and quadratic cost coefficient of the  $i^{th}$  generator;
- $P_{Gi}$  is the active power output of the  $i^{th}$  generator:

$$FC_{it}(P_{G,it}) = a_i \times P_{G,it}^2 + b_i \times P_{G,it} + c_i \quad (3)$$

where  $a_i$ ,  $b_i$ ,  $c_i$  are the fuel cost coefficients for the  $i^{th}$  unit.

### b: QUADRATIC FORM WITH VALVE POINT EFFECTS

Since it is important to consider the valve-point effects to obtain a more accurate model, the cost function can be modified to include the ripple curve created by valve-point effect as follows:

$$FC_{it}(P_{G,it}) = a_i \times P_{G,it}^2 + b_i \times P_{G,it} + c_i + \left| e_i \times \sin(f_i \times (P_{G,i}^{\min} - P_{G,it})) \right| \quad (4)$$

where  $e_i$ ,  $f_i$  are cost coefficients, and  $P_{G,i}^{\min}$  is the minimum output of the  $i^{th}$  unit.

### 2) REAL POWER RE-DISPATCH COST

Real power generation re-dispatch cost (GRC) across the entire decision horizon can be formulated as follows:

$$GRC = \sum_{i \in N_G} (c_{it}^u P_{G,it}^u + c_{it}^d P_{G,it}^d) \forall t \quad (5)$$

where

- $P_{G,it}^u$  and  $P_{G,it}^d$  are the increased and decreased in active power generation of unit  $i$  at time  $t$ , respectively;
- $c_{it}^u$  and  $c_{it}^d$  are cost of increase and decrease in active power generation of unit  $i$  at time  $t$ , respectively.

### 3) REAL POWER PROCUREMENT COST

The power procurement cost function is usually used in reserve necessary for real-time re-dispatch decision-making.

$$\text{Minimize } \sum_{i=1}^{N_{G_p}} P_{pi} \lambda \quad (6)$$

where

- $N_{G_p}$  is the number of generators in the power market pool;
- $\lambda$  is the electricity price (in \$/kWh);
- $P_{pi}$  is the real power purchased from pool by the  $i^{th}$  generator.

4) REACTIVE POWER GENERATION COST

Cost of reactive power generation  $CQ_{G,i}$  can be formulated as:

$$\begin{aligned}
 CQ_{G,i} &= \sum_{i \in NG} (a_Q * Q_{G,i}^2 + b_Q * Q_{G,i} + c_Q) \\
 &= \sum_{i \in NG} (a_i * \sin^2 \theta * Q_{G,i}^2 + b_i * \sin \theta * Q_{G,i} + c_i)
 \end{aligned}
 \tag{7}$$

where  $a_Q, b_Q, c_Q$  are reactive power cost coefficients and these coefficients are determined from  $a_i, b_i, c_i$ , i.e., the active power cost coefficients by modified triangle method.

Other than the cost for generation plants, cost associated with shunt capacitors such as SVC and other reactive power providers such as FACTS devices can also be included.

$$\begin{aligned}
 \text{Minimize } C_Q &= \sum_{i=1}^{NG} C_{Qi} + \sum_{j=1}^{NC} C_{SVCj} + \sum_{k=1}^{NF} C_{FACTSk} \\
 C_{Qi} &= a_i + b_i Q_i \\
 C_{SVCj} &= a_j + b_j Q_j + c_j Q_j^2 \\
 C_{FACTSk} &= a_k + b_k Q_k + c_k Q_k^2
 \end{aligned}
 \tag{8}$$

where

- $NG$  is the number of generators including the slack generators in the network;
- $NC$  is number of shunt capacitor in the network;
- $NF$  is the number of FACTS devices in the network;
- $a_i, b_i$  are the basic and linear cost coefficient of the  $i^{th}$  generator;
- $a_j, b_j, c_j$  are the basic, linear and quadratic cost coefficient of the  $j^{th}$  capacitor;
- $a_k, b_k, c_k$  are the basic, linear and quadratic cost coefficient of the  $k^{th}$  FACTS device;
- $Q_i, Q_j, Q_k$  is the reactive power output of the  $i^{th}$  generator, the  $j^{th}$  capacitor and the  $k^{th}$  FACTS device, respectively.

Another way to consider reactive power generation cost is by considering the opportunity cost. The opportunity cost of using a resource for one purpose is defined as the benefit lost by not being able to use in another (or at another time) alternative way. For example, a generator has to decrease active power production because of its reactive power needs which will in turn reduce the opportunity of obtaining profits from the active power market. The profit of decreased active power production (implicit financial loss to generator) is modeled as the reactive power opportunity cost.

A simple model for opportunity cost is as below:

$$f_{q,i}(Q_{G,i}) = [f_{p,i}(S_{G,i}^{\max}) - f_{p,i}(\sqrt{S_{G,i}^{\max 2} - Q_{G,i}^2})] * r_{G,i}, \tag{9}$$

where

- $Q_{G,i}$  is the reactive power output of generator  $i$ ;
- $S_{G,i}^{\max}$  is the maximum apparent power of generator  $i$ ;
- $f_{p,i}(\cdot)$  is the active power cost, which is modeled as a quadratic function;
- $r_{G,i}$  is an assumed profit rate for active power generation  $i$ .

5) REACTIVE POWER PROCUREMENT COST

Reactive power in the power systems usually comes from three sources: from generators, capacitors, and from line charging reactive resources.

We assume that the reactive compensators are static capacitors owned by private investors and installed at some selected buses. The charge for using capacitors can be assumed to be proportional to the amount of the reactive power output purchased and can be expressed as:

$$CQ_{C,j} = r_{C,j} * Q_{C,j} \tag{10}$$

where  $r_{C,j}$  and  $Q_{C,j}$  are the reactive price and amount purchased, respectively.

An alternative formulation of  $CQ_{C,j}$  is as below:

$$CQ_{C,j} = \frac{c_C * Q_{C,j}}{\text{lifespan} * \text{usage}} \tag{11}$$

where  $c_C$  is capital investment cost of the capacitor per MVar.

Cost for the line charging reactive sources  $CQ_{Ch,k}$  can be formulated as:

$$CQ_{Ch,k} = r_{Ch,k} * Q_{Ch,k} \tag{12}$$

where  $r_{Ch,k}$  is per unit cost of reactive power supplied by line charging which is assumed to be equal to the average per unit cost of all reactive power sources present in the system.

$Q_{Ch,k}$  is the total reactive power supplied by line charging and is formulated as:

$$\begin{aligned}
 Q_{Ch,k} &= \sum_{n \in N_B} \sum_{m \in \Omega_n} Q_{Ch,nm} \\
 &= \sum_{n \in N_B} \sum_{m \in \Omega_n} (V_n^2 \frac{y_{Ch,nm}}{2} + V_m^2 \frac{y_{Ch,nm}}{2})
 \end{aligned}
 \tag{13}$$

where  $V_n$  and  $V_m$  are voltage magnitudes at the end bus  $n$  and  $m$ , and  $y_{Ch,nm}$  is line charging admittance of branch  $nm$ .

6) ACTIVE/REACTIVE POWER RESCHEDULE

Active/Reactive power reschedule is usually used in security-constrained OPF to stabilize the contingencies that will threaten the power system stability.

Active power reschedule can be formulated as below:

$$\Delta P_G = \sum_{i \in \Omega_G} (P_{G,i} - P_{G,i}^0)^2 \tag{14}$$

where  $P_{G,i}^0$  is the initial active power generation at generator  $i$ , and  $P_{G,i}$  is the active power generation after the re-dispatching. Reactive power reschedule amount can be formulated similarly.

7) REACTIVE POWER GENERATION

Due to the increasing demand and insufficient generation capacity expansion, voltage stability has become a major concern in power system planning and operation. Reactive power generation is critical in maintaining the voltage levels. Therefore, it is of paramount importance to present sufficient amount of reactive power generation to secure and guarantee

the reliable operation of power system. One way to maximize the system reactive power generation is to maximize systems inherent reactive power generation, i.e., to maximize the line charging reactive power output

$$\text{Maximize } Q_{ch} = \sum_{ij=1}^{N_{br}} Q_{C_{ij}} \quad (15)$$

$$Q_{C_{ij}} = V_i^2 \frac{Y_{C_{ij}}}{2} + V_j^2 \frac{Y_{C_{ij}}}{2} \quad (16)$$

where  $Q_{C_{ij}}$  is reactive power supplied by line charging of branch  $ij$ .

### 8) REAL POWER RESERVE COST

The United States Federal Energy Regulatory Commission (FERC) defines the ancillary services as: “those services necessary to support the transmission of electric power from seller to purchaser given the obligations of control areas and transmitting utilities within those control areas to maintain reliable operations of the interconnected transmission system.”

Real power reserves, such as spinning reserves, non-spinning reserves and ramp-up/down reserves, are important form of ancillary services that support the re-dispatching and regulations under *load fluctuation, renewable energy uncertainty and possible contingencies*.

An example formulation for ancillary service cost, considering up-ramp, down-ramp, spinning and non-spinning reserve cost is as below:

$$\begin{aligned} ASC = & \sum_{i \in I_{RU}} f_{u,i}(R_{u,i}) + \sum_{i \in I_{SP}} f_{s,i}(R_{s,i}) \\ & + \sum_{i \in I_{NS}} f_{n,i}(R_{n,i}) + \sum_{i \in I_{RD}} f_{d,i}(R_{d,i}) \end{aligned} \quad (17)$$

where

-  $f_{d,it}(\cdot), f_{u,it}(\cdot), f_{s,it}(\cdot), f_{n,it}(\cdot)$  represent the cost of generating unit  $i$  at time  $t$  for down-ramp, up-ramp, spinning and non-spinning reserve, respectively;

-  $R_{d,i}, R_{u,i}, R_{s,i}, R_{n,i}$  represent the reserve amount of generating unit  $i$ ;

-  $I_{RU}, I_{SP}, I_{NS}, I_{RD}$  represent the set of generators providing up-ramp, spinning and non-spinning, down-ramp reserve, respectively.

### 9) REACTIVE POWER RESERVE (COST)

Reactive power reserve is another important ancillary service in the electric systems, which provide the ability to produce or absorb reactive power and maintain the voltage level of the system. Example formulations are as follows:

$$Q_{res}^{max} = \sum_{i \in N_G} w_i * Q_{res,i}^{max} \quad (18)$$

$$Q_{res,i}^{max} = Q_{G,i}^{max} - Q_{G,i} \quad (19)$$

where

-  $Q_{res}^{max}$  is the sum of reactive reserves of the system to be optimized;

-  $Q_{res,i}^{max}$  is the reactive reserve of the  $i$ -th generator, which is the difference between the maximum reactive generation  $Q_{G,i}^{max}$  and reactive power dispatched  $Q_{res,i}$ ;

-  $w_i$  is the weight factor of the  $i$ -th generator.

### 10) LOAD SHEDDING

Load shedding is a signal that the system is not able to meet the load requirements. Minimizing load shedding can be seen as a reliability objective and can be formulated as:

$$\text{Minimize } \sum_d^{ND} L_d^{SH} \quad (20)$$

where

-  $ND$  is the number of loads in the network;

-  $L_d^{SH}$  is the load shedding at load  $d$ .

Amount of load shedding can be represented with load shedding factors, formulated as below:

$$\sum_{n \in N_B} P_{L,n} * \theta_n \quad (21)$$

where  $P_{L,n}$  is active and reactive loads at bus  $i$ , and  $\theta_n$  represents the fraction of load curtailed in the bus.

### 11) LOAD SHEDDING COST

According to the load controlling scheme, load shedding always comes with cost, which may come from the economic damage to the costumers or the price paid based on contract. Quadratic formulation of load shedding cost is as follows:

$$\sum_{i=1}^{N_L} (p'_i + q'_i L_{shd,i} + r'_k L_{shd,i}^2) \quad (22)$$

where

-  $p'_i, q'_i$  and  $r'_k$  are cost coefficients of load shedding at load  $i$ ;

-  $L_{shd,i}$  means the amount of load shed at load  $i$ .

Under the circumstances when contacts with customers should be followed in terms of the maximum amount of load to shed and the load shedding price, the following formulation is available:

$$CL_{sh} = \sum_{i \in N_L} \sum_{kt} [X_{ki}^t \cdot PC1_{ki}^t + U_{ki}^t \cdot PC2_{ki}^t] \cdot CC_k \quad (23)$$

where

-  $CC_k$  is the curtailment cost of customer type  $k$ ;

-  $PC1_{ki}^t$  is the maximum curtailable MW at 1-hour notice of type  $k$  at  $t$  at bus  $i$ ;

-  $PC2_{ki}^t$  is the maximum curtailable MW at 1-day notice of type  $k$  at  $t$  at bus  $i$ ;

-  $X_{ki}^t$  is the level of curtailable load selection of type  $k$  at  $t$  at bus  $i$  at 1-hour notice (0 to 1). It is assumed that, with 1-hour notice, the load curtailment duration is shorter and is limited to time-period  $t$ ;

-  $U_{ki}^t$  is the level of curtailable load selection of type  $k$  at  $t$  at bus  $i$  at 1-day notice (0 to 1). It is assumed that with 1-day advance notice, the customers can shift their load for longer duration and it would give a MW and MVA<sub>r</sub> reduction for a fixed number of hours  $S$ ;

-  $k$  represents the type of curtailable load by customer class e.g. agricultural, industrial etc. (based on power factor and curtailment cost of customers)

### 12) LOAD SHEDDING BENEFIT

Load shedding, as a form of control to the operators, can be beneficial to the system as a whole. A possible way to describe the load shedding benefit is as below:

$$\sum_i \sum_{Type} (CL \cdot \lambda_i \cdot \Delta PD_{i,Type}) \quad (24)$$

where  $CL$  denotes the cost of lost load (dollars per MW hour) and when multiplied with  $\lambda_i$  and  $\Delta PD_{i,Type}$  denotes the ISO's benefit from demand reduction at a bus. Evidently, the gross economic value of loss reduction from load curtailment depends on location of load reduction, given by  $\lambda_i$ .

### 13) SUPPLIED LOAD

Another approach to limit the load shedding quantity in order to maximize the customer benefit is to maximize the load to supply. The amount of supplied load can be represented by load factor:

$$\sum_{n \in N_B} \alpha_n \quad (25)$$

where  $\alpha_n$  is the load factor at bus  $n$  having existing load. The load factor  $\alpha_n$  can be an optimization variable which enables maximizing the picked-up load at the end of the optimization process.

### 14) NUMBER OF CONTROL ACTIONS

Control actions in the system are associated with cost, which can come from the degradation of the control devices, the maintenance fee, the initial capital investment and the operational cost of executing the control signal. As a result, to reduce the number of control actions is an objective for the utilities.

One way to model the number of controllable devices uses the control variable status indicator that is associated with each control variable. The formulation is as below:

$$NC = \sum_{i=1}^{N_{control}} s_i \quad (26)$$

where  $s_i$  represents control variable status, with 1 indicates a control action and 0 meaning no action.

### 15) SHIFT OF CONTROL ACTIONS

The magnitude of a control variable shift is another concern of the utilities, and has appeared as an objective in the literature. An example formulation of the shift of control actions is as below:

$$\sum_{i=1,TP} [W_{itp} \cdot (T_i - T_i^0)^2] + \sum_{i=1,PS} [W_{ips} \cdot (A_i - A_i^0)^2] + \sum_{i=1,CP} [W_{icp} \cdot (B_i - B_i^0)^2] \quad (27)$$

where

- $T_i^0$  and  $T_i$  are transformer tap position before and after the optimization, respectively;
- $A_i^0$  and  $A_i$  are phase shifter angle before and after the optimization, respectively;
- $B_i^0$  and  $B_i$  are shunt capacitor susceptance before and after the optimization, respectively;
- $W_{itp}$ ,  $W_{ips}$ ,  $W_{icp}$  are weight factors associated each class of control.

### 16) SYSTEM LOADABILITY

Loadability is a measure of the efficient use of transmission lines in the system. Average loadability on all transmission lines can be viewed as a system security index, formulated as follows:

$$Average\ Loadability = \frac{1}{n_T} \sum_{l=1}^{n_T} \frac{S_l}{S_l^{max}} \quad (28)$$

where

- $n_T$  is the number of transmission lines;
- $S_l$  is the apparent power on line  $l$ ;
- $S_l^{max}$  is the maximum apparent power on line  $l$ .

In the function above, the apparent power on transmission line  $l$  includes from the sending end to the receiving end,  $S_{lf}$ , and the apparent power from the receiving end to the sending end,  $S_{lr}$ . Therefore, in the objective function, it is defined that

$$S_l = \frac{1}{2}(S_{lf} + S_{lr}) \quad (29)$$

The formulation of transmission line loadability can be further modified to consider only the highly loaded lines [26].

### 17) VOLTAGE STABILITY

When representing the voltage stability constraint explicitly, voltage stability indices are usually used. For example,

$L$ -index:

$$L_{max} = \max(L_i) \text{ and } L_j = \left| 1 - \sum_{i=1}^g F_{ji} \left( \frac{V_i}{V_j} \right) \right| \quad (30)$$

where  $i = 1, 2, \dots, g$  are the generator buses and  $j = g + 1, g + 2, \dots, n$  are the load buses,  $F_{ji}$  is obtained from Y bus matrix. The load bus corresponding to highest  $L$ -index highlights the most critical bus and therefore  $L_{max}$  can be a metric for the proximity of the system to voltage collapse point. Minimizing  $L_{max}$  for different operating conditions will identify those for which for which system is most stable.

Voltage collapse point index (VCPI):

The VCPI was proposed by Moghavvemi and Faruque which is based on the concept of maximum power transferred through the lines of the network:

$$VCPI(power) = \frac{P_r}{P_{r(max)}} = \frac{Q_r}{Q_{r(max)}} \quad (31)$$

$$P_{r(max)} = \frac{V_s^2 \cos \phi}{Z_s 4 \cos^2((\theta - \phi)/2)} \quad (32)$$

$$Q_{r(\max)} = \frac{V_s^2}{Z_s} \frac{\sin \phi}{4\cos^2((\theta - \phi)/2)} \quad (33)$$

where

-  $P_r$  and  $Q_r$  are the real and reactive power transferred to the receiving end and it is obtained from the power flow calculations;

-  $P_{r(\max)}$  and  $Q_{r(\max)}$  are the maximum active and reactive power that can be transferred through a line;

-  $V_s$  is the sending end voltage;

-  $Z_s$  is the line impedance;

-  $\theta$  is the line impedance angle;

-  $\phi = \tan^{-1}(Q_r/P_r)$  is the phase angle of the load impedance.

Voltage stability can also be formulated with an optimization problem which maximizing the load margin between the base case load and the voltage collapse point. Voltage stability can also be represented implicitly by an external problem.

## 18) CONSTRAINT VIOLATION

The number of constraint violations or the severity of violations can be considered in objective for problems such as system restoration, corrective control optimization and worst case scenario identification. Constraint violation can be formulated as below:

$$Violation = \sum_{i \in N_{Con}} \delta_i \quad (34)$$

where  $N_{Con}$  is the set of constraints, and  $\delta_i$  can represent either the violation status or as the relaxation variable of the  $i^{th}$  constraint.

## 19) SYSTEM POWER IMBALANCE

The system power imbalance is defined as the sum over all buses of the absolute value of nodal power balance violations. The absolute value is modeled in a linear fashion by two sets of non-negative variables  $\Delta P_n$ :

$$Imbalance = \sum_{n \in N_B} (\Delta P_n) \quad (35)$$

$$P_{inj,n} = P_{G,n} - P_{L,n} - \Delta P_n \quad (36)$$

where

-  $P_{inj,n}$  is the power injection at bus  $n$ ;

-  $P_{G,n}$  and  $P_{L,n}$  are generation and load at bus  $n$ , respectively;

-  $N_B$  is the set of buses.

## 20) SECURITY RISK

Security risk can represent the probable financial impact of the event assuming the given condition. As an example, consider risk calculation of voltage collapse. Voltage instability is usually triggered by load parameter variations, transmission system contingency and generator unit outage which lead to reactive power deficiency. The probability of voltage collapse can be formulated as:

$$P_r(\text{coll}) = \left[ \sum_{E_i} \Pr(\text{coll}E_i) \times \Pr(E_i) \right]$$

$$+ \left[ \sum_{G_i} \Pr(\text{coll}G_i^{\text{out}}) \times \Pr(G_i^{\text{out}}) \right] \quad (37)$$

where  $\Pr(\text{coll}E_i)$  and  $\Pr(\text{coll}G_i^{\text{out}})$  are the probability of voltage collapse under a given contingency  $E_i$  and a given generator outage  $G_i^{\text{out}}$ , respectively.

The impact of voltage instability is reflected through the interruption cost (loss) of system loads due to local or system-wide voltage collapse. For cost of load interruption a uniform price per MW can be adopted, though or more sophisticated forms have been proposed, e.g., individual bus specific or even duration dependent cost (loss) function across the system. The severity of the event over the affected area is calculated as

$$Severity = \sum_{bus} (Interrupted)_{bus} \times (Associated\ Interruption\ Cost) \quad (38)$$

The risk of voltage collapse for the conditions presented above is calculated by providing its severity beside associated probability [70], [79], as below:

$$Risk = Probability * Severity \quad (39)$$

## 21) POWER LOSSES

Minimizing active power losses is a common objective used in power system optimization. Two forms of formulations are available:

*System* : Total power losses equals to total power generation minus total load network:

$$P_{Loss} = \sum_{i=1}^{N_G} P_{G_i} - \sum_{j=1}^{N_L} P_{L_j} \quad (40)$$

where  $i$  and  $j$  are the bus numbers in the range of  $1 - N$ .

An example of detailed formulation considering various kinds of loss is as follows (considering AC, DC transmission lines and voltage source converter (VSCs)):

$$P_{LOSS} = P_{acloss} + P_{dcloss} + P_{vscloss} \quad (41)$$

with the following components:

- AC transmission losses:

$$P_{acloss} = 0.5 \sum_{n=1}^{N_B} \sum_{m=1}^{N_B} g_{nm} (V_n^2 + V_m^2 - 2V_n V_m \cos(\delta_n - \delta_m)) \quad (42)$$

- DC transmission losses:

$$P_{dcloss} = 0.5 \sum_{n_{dc}=1}^{M_B} \sum_{m_{dc}=1}^{M_B} g_{n_{dc}m_{dc}} (V_{n_{dc}} - V_{m_{dc}})^2 \quad (43)$$

- Active power losses of VSCs:

$$P_{vscloss} = \sum_{i=1}^{M_B} (A_{li} + B_{li}I_{vi} + C_{li}I_{vi}^2) \quad (44)$$

$$(I_{vi}V_{ci})^2 = P_{ci}^2 + Q_{ci}^2 \quad \forall i \in M_B \quad (45)$$

where

- $g_{nm}$  is the conductance of the line  $nm$ ;
- $M_B$  is the set of all DC buses;
- $A_{li}, B_{li}, C_{li}$  are VSC loss coefficient of VSC  $i$ ;
- $I_{vi}$  is phase current of VSC valve of VSC  $i$ ;
- $V_{ci}, P_{ci}, Q_{ci}$  are voltage magnitude, active power and reactive power at VSC ac bus.

Minimizing reactive power losses is also considered in the OPF formulations, since reactive power is very important in supporting power transmission and system security. Followed is a possible formulation:

$$\text{Minimize } Q_{loss} = \sum Q_{Gi} - \sum Q_{Di}, \quad i = 1, \dots, N_b \quad (46)$$

where  $Q_{Gi}, Q_{Di}$  are the reactive power generation and demand at bus  $i$ , respectively.

## 22) POWER TRANSFER CAPABILITY

Available transfer capability (ATC), as a measure of the transfer capability remaining in the physical transmission network with respect to system security and stability, can be formulated as the maximum power the system can transmit from sources (generations) to sinks (loads). When viewing ATC or total transfer capability (TTC) as objective, there are possible formulations as follows:

$$\min f(t) = -\lambda \sum_{i \in S_L} b_{Pi} \quad (47)$$

where

- $\lambda$  is the parameter controlling the amount of load increment;
  - $S_L$  is the node set in sink area;
  - $b_{Pi}$  is the real power load of the sink node  $i$ .
- ATC for prescribed interfaces can be represented by:

$$ATC = \sum_{l=1}^{N_{TIE}} (P_l^* - P_l) \quad (48)$$

where  $N_{TIE}$  is the number of tie lines across the interface, in which the active powers share the same prescribed direction; and  $P_l$  is the active power-flow of tie line  $l$ . Variables with subscript \* represent those at the critical equilibrium point, while variables without subscript \* denote those at the current operating point.

ATC for the entire system can also be formulated as the maximum loading distance:

$$ATC = \sum_{i \in Sink} (P_{Di}(\lambda^*) - \sum_{i \in Sink} P_{Di}(\lambda^0))$$

or  $ATC = \lambda^* - \lambda^0 \quad (49)$

where  $\lambda$  is the scalar parameter representing the increase in bus load or generation.  $\lambda^0$  corresponds to the base case and  $\lambda^*$  corresponds to the maximal transfer.  $\sum_{i \in Sink} (P_{Di}(\lambda))$  is sum of load at sink area corresponds to  $\lambda$ .

## 23) LOOP FLOW

Loop flow, also called transit flow, parallel path flow or circulating flow, refers to the fact that the power can flow through several paths in a meshed network. Unscheduled loop flow becomes a concern when it adds to the loading of inner and interconnection transmission lines and endangers security, moving the system to insecure state or even emergency state.

A way to formulation loop flow is as follows. Consider a system exchanging power with the remaining of the interconnection through  $N_{TIE}$  tie-line, in which the active power  $p_l$  are counted positively when exiting the system. Intuitively, there is a loop flow if some lines are bringing power in and some others are taking it out. This means that not all  $p_l$  have the same sign, which leads to the formulation as below:

$$LF = \frac{1}{2} \left( \sum_{l=1}^{N_{TIE}} |p_l| - \left| \sum_{l=1}^{N_{TIE}} p_l \right| \right) \quad (50)$$

where  $N_{TIE}$  is the set of tie lines.

## 24) DEMAND BENEFIT

When considering demand side management (DSM), demand benefit can be an important optimization objective. Following is an example formulation considering both demand benefit and generation cost:

$$\text{maximize } [f(x, u) = \sum_{c=1}^{N_c} B_c(d) - \sum_{g=1}^{N_g} C_g(s)] \quad (51)$$

$$B_c(d) = B_c(d_p, d_q) = B_{pc}(d_p) + B_{qc}(d_q) \quad (52)$$

$$C_g(s) = C_g(s_p, s_q) = C_{pg}(s_p) + C_{qg}(s_q) \quad (53)$$

where

- $N_c, N_g$  are the set of pool load buses and the set of pool generator buses, respectively;
- $d, s$  are the demand vector and supply vector, respectively;
- $B_c(d), C_g(s)$  are the benefit of consumer  $c$  and the cost of supplier  $g$ ;
- Production costs and demand benefit functions are quadratic functions of active and reactive power of loads and generators, as follows:

$$C_{pg}(s_p) = a_{0g} + a_{1g}s_{pg} + a_{2g}s_{pg}^2 \quad (54)$$

$$C_{qg}(s_q) = a_{0g} + a_{1g}|s_{qg}| + a_{2g}s_{qg}^2 \quad (55)$$

$$B_{pc}(d_p) = b_{0c} + b_{1c}d_{pc} + b_{2c}d_{pc}^2 \quad (56)$$

$$B_{qc}(d_q) = -B_{q0c}[d_{qc} - \gamma d_{pc}]^2 \quad (57)$$

## 25) SOCIAL WELFARE

Social welfare means the benefit of all the participants, i.e. consumers and producers surplus, which can be formulated as:

$$\text{Social Welfare} = \sum_{i \in C} B_i(x_i) - \sum_{j \in G} C_j(x_j) \quad (58)$$

where  $C(x)$  is the cost function of production that represents the producers, which could include the cost associate with

real and reactive power generation, reserve capacity, load shedding, and so on. And  $B(x)$  is the benefit function of consumption at quantity  $x$  that represents the consumers, which can be modelled by a quadratic function.

26) ENVIRONMENTAL IMPACT

The emission function can be presented as the sum of all types of emissions considered, such as  $NO_x$ ,  $SO_x$ , thermal emission, etc. The amount of  $NO_x$  and  $SO_x$  emission, which is given as a function of generator output that is the sum of a quadratic and exponential function, is considered in the following formulation:

$$EC = \sum_{i \in N_G} \sum_{t \in T} (\alpha_i * P_{G,it}^2 + \beta_i * P_{G,it} + \gamma_i + \zeta_i \exp(\lambda_i * P_{G,it})) \quad (59)$$

where  $\alpha_i$ ,  $\beta_i$ ,  $\gamma_i$ ,  $\zeta_i$  and  $\lambda_i$  are emission coefficients for the  $i$ -th unit.

27) NUMERICAL EVALUATIONS

In this section, the IEEE RTS power system is used to demonstrate the impact of different objective functions on the AC OPF results. For this aim, first, some indices are introduced to calculate the effectiveness of the OPF results in terms of different power system aspects including generation cost, voltage index, power loss, lost loads, environmental impacts. Furthermore, a multi-period AC OPF is formulated in GAMS and solved considering various objective functions introduced in previous sections. The results are given in Table 3, where, VI is voltage index and given by (60) [89].

$$VI = \sum_{i=1}^{N_{bus}} \left( \sum_{t=1}^{N_t} (V_n^* - V_{it})^2 \right) \quad (60)$$

where  $i$  refers to the system bus,  $t$  indicates the time period,  $N_{bus}$  and  $N_t$  are the number of buses and time periods, respectively. Generation cost is calculated by (2). Power loss index (PLI) represents the real power loss of the system and is calculated as shown in (61).

$$PLI = \sum_{i=1}^{N_{bus}} \sum_{j \neq i}^{N_{bus}} \sum_{t=1}^{N_t} (P_{ij,t} + P_{ji,t}) \quad (61)$$

For all  $i \neq j$  if  $ij$  are connected.

where  $P_{ij}$  is the power flowing the line between bus  $i$  and bus  $j$ . Since the signs are different, the sum of them (difference of them) is equal to the line loss. Furthermore, lost load index (LLI) refers to not supplied loads and is calculated by (20). Finally, the environment index (EMI) is the impact of the generation units on the air pollution given in (59). The emission coefficients of the proposed test case are given in Table 4.

Shown in Table 3, the voltage index as one of the important technical and functional characteristics of the power system highly depends on the objective function of OPF. Fig. 3 shows that considering the voltage-related objective functions

TABLE 3. Comparison of Performance under Various objective functions in the OPF solution.

Objective function	Performance index						
	VI	Gen. Cost (\$)	PLI	LLI	EMI	Iteration	Sim. time
Active generation cost (linear)	2.159	363571.172	1864.603	13744.552	526.66	1153	2.344
Active generation cost (nonlinear)	2.163	363571.172	1903.864	12187.97	526.66	1179	2.328
Active generation cost with valve	2.234	363571.172	1903.626	12112.331	526.66	1275	2.343
Reactive power generation cost	3.268	787062.12	1924.417	4744.785	1.14E+09	1402	2.344
Load shedding and load shedding cost	1.778	968262.195	1451.713	0	347517.483	1147	2.688
Voltage quality	0.082	472747.175	3933.439	12775.329	567.631	1190	2.407
Active power loss	4.714	463810.098	174.044	3487.89	1144.878	1357	2.328
Environmental impact	1.908	432320.273	1650.27	9587.695	432.205	1202	2.344

TABLE 4. Assumed emission coefficients for generation units in IEEE RTS.

	G <sub>1</sub>	G <sub>2</sub>	G <sub>3</sub>	G <sub>4</sub>	G <sub>5</sub>	G <sub>6</sub>	G <sub>7</sub>	G <sub>8</sub>	G <sub>9</sub>	G <sub>10</sub>
$\gamma$	0.05638	0.05638	0.06490	0.06490	0.06490	0.03380	0.04586	0.04586	0	0.03380
$\beta$	-0.06047	-0.06047	-0.05554	-0.05554	-0.05554	-0.03550	-0.05094	-0.05094	0	-0.03550
$\alpha$	0.02543	0.02543	0.04091	0.04091	0.04091	0.05326	0.04258	0.04258	0	0.05326
$\zeta$	0.0005	0.0005	0.0002	0.0002	0.0002	0.002	0.000001	0.000001	0	0.002
$\lambda$	3.333	3.333	2.857	2.857	2.857	2.000	8.000	8.000	0	2.000

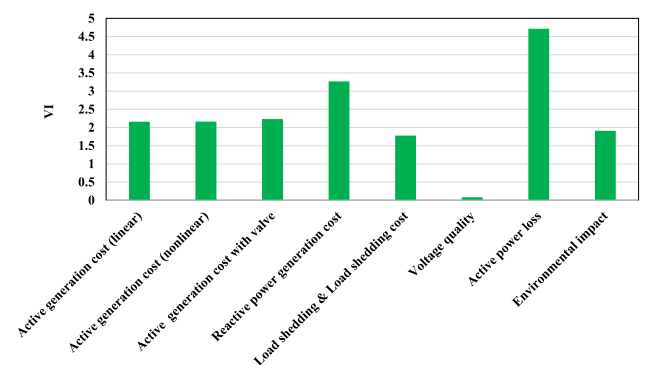


FIGURE 3. The impact of various OPF objective functions on voltage index.

can significantly improve this voltage index. The real power generation cost and the lost load index can be considered almost opposite to each other. In other words, generation cost is based on reducing unit generations to reduce the costs, while the lost load index is based on increasing the generation of the units to supply all system loads taking into account the equality and inequality constraints. Fig. 4 shows the change in generation cost and lost load index through changing the objective functions. According to Fig. 4, it is evident that, although generation cost-based objective functions have approximately the same generation cost, the amount of the lost load decreased by considering the cost effects of the valve. The load-shedding-based objective functions set the lost load at zero but increased the generation cost dramatically.

The presented data in Table 3 show that the reactive power generation cost objective function has a negative

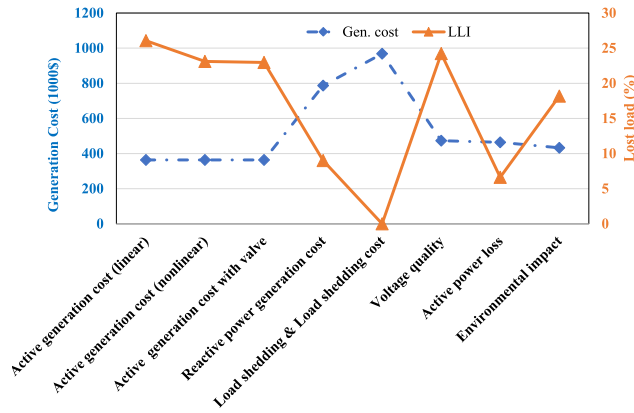


FIGURE 4. The impact of various OPF objective functions on generation cost and lost load.

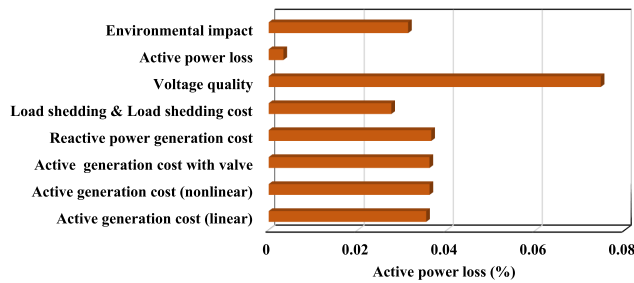


FIGURE 5. The impact of various OPF objective functions on active power loss.

effect on many power system performance indices. In other words, although it improved the lost load index, it extremely increases the generation cost, voltage index, active power loss, and air emissions. The impact of the various OPF objective functions on the total active loss of the power system is shown in Fig. 5. It can be seen that the active power loss is almost in the same range for different objective functions except for voltage quality and power loss objective functions. It can be concluded that the voltage quality objective function is the worst and active power loss is evidently the best objective function in terms of real power loss in the power system planning through OPF.

Finally, in terms of computation burden and the number of iterations, almost all the objective functions have the same performance. Therefore, selecting the OPF objective function doesn't have a critical impact on the computation time of the simulation.

**B. CONVENTIONAL CONTROL VARIABLES**

Fig. 6 shows a categorization of the conventional control variables found in literature, including traditional controls, uncertainty-related controls, load & storage-related controls, and transmission devices-related controls. Tables 5-8 summarize the conventional control variables found in corresponding literature with references, and the

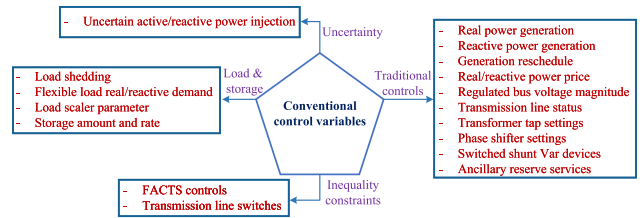


FIGURE 6. Categorization of conventional control variables.

TABLE 5. Categories of uncertainty-related control variables with references.

Variable	Type(s)	References
Uncertain active/reactive power injection	Continuous	[69]

TABLE 6. Categories of transmission devices related control variables with references.

Variable	Type(s)	References
FACTS controls	Continuous, Discrete	[23]–[26]
Transmission line switches	Binary	[13]

TABLE 7. Categories of load and storage related control variables with references.

Variable	Type(s)	References
Load Shedding	Continuous, Discrete	[22], [33], [48], [49], [53], [54], [58], [62]–[64], [88]
Flexible load real/reactive demand	Continuous	[53], [56], [59], [74], [75], [81], [85]
Load scalar parameter	Continuous	[74], [75]
Storage amount and rate	Continuous	[38]

control variable types of being continuous, discrete or binary are considered as well.

**C. CONVENTIONAL CONSTRAINTS**

The OPF solves the economic dispatch problem by adding additional constraints to the optimization problem. The key addition to the economic dispatch problem is the inclusion of network constraints, which are categorized into two types: equality constraints and inequality constraints. Fig. 7 shows the categorization of the conventional constraints found in the literature. Table 9 summarizes the conventional constraints found in the literature with references.

According to the categories from Fig. 7 and Table 9, the detailed mathematical formulas and explanations under each specific conventional objective function are further given and shown as follows.

TABLE 8. Categories of traditional control variables with references.

Variables	Type(s)	References
Real power generation	Continuous	[21]–[24], [30]–[41], [44], [47]–[55], [58], [59], [63], [74], [75], [78], [81]–[83], [85], [87], [88], [88], [90]–[98]
Reactive power generation	Continuous	[32], [33], [35]–[38], [40], [42], [44], [51], [52], [56]–[59], [71], [71], [78], [82], [83], [91]–[100]
Generation reschedule	Continuous	[30], [45], [50]–[54]
Real/reactive power price	Continuous	[82]
Regulated bus voltage magnitude	Continuous	[20], [21], [34], [45], [55], [60], [61], [71], [90], [98], [99]
Transformer tap settings	Discrete, Continuous	[20], [21], [34], [35], [57], [58], [60], [71], [81], [87], [90], [94], [98], [99]
Phase shifter setting	Discrete, Continuous	[58], [87]
Switched shunt Var devices	Discrete, Binary, Continuous	[20], [21], [34], [35], [49], [52], [57], [60], [64], [71], [87], [90], [98]
Auxiliary service reserves (spinning, non-spinning, reactive power, ramping)	Continuous	[31], [33], [45], [48], [53], [61], [63], [82], [92], [99]
Transmission line status	Binary	[37], [40]

TABLE 9. Conventional OPF constraints with references.

Equality Constraints	
Constraints	References
Full AC power flow	[13], [21], [22], [25], [26], [30]–[37], [39], [41], [43]–[45], [47], [48], [50]–[53], [55]–[65], [69], [74], [75], [82], [83], [87], [88], [90]–[92], [94]–[97], [99]
DC power flow	[24], [30], [40], [42], [54], [85]
AC-DC converter equations	[43], [45], [98]
Generator dynamic equations	[36], [39], [65], [78], [91], [93], [94], [96], [101]
Inequality Constraints	
Generation & Ancillary Service Related	
Constraints	References
Real/reactive power generation limits	[22], [23], [30]–[38], [40]–[45], [47], [51]–[55], [57], [59], [61], [63]–[65], [74], [75], [78], [82], [83], [85], [87], [88], [90], [91], [93]–[99]
Generation contract	[64], [92]
Generation ramping limits	[22], [30], [31], [33], [34], [42], [50], [52]–[54], [59], [77], [85], [90], [95], [97], [99]
Real/reactive power reserve consuming limits	[31], [42], [45], [46], [48], [53], [61], [63], [64], [82], [92], [100]
Demand Related	
Constraints	References
Load shedding limits	[22], [33], [63], [64], [87]
Flexible demand limits	[31], [42], [45], [46], [48], [53], [61], [63], [64], [82], [92], [100]
Control Devices Related	
Constraints	References
Shunt capacitor limits	[20], [21], [31], [34], [35], [57], [60], [64], [90], [98]
Transformer tap limits	[20], [21], [34], [35], [57], [62], [87], [90], [94], [98]
Phase shifter angle limits	[58], [68], [87]
FACTS device constraints	[23], [24], [26], [43], [95]
Number of control actions limits	[37], [49], [63], [67]
System Operational Security Related	
Constraints	References
Bus voltage limits	[20]–[26], [30], [31], [33]–[37], [41], [43]–[45], [47], [51]–[53], [56], [57], [59]–[61], [63]–[65], [69], [74]–[76], [78], [82], [83], [85], [87], [88], [88], [90]–[101]
Branch flow limits	[21]–[24], [26], [30], [32]–[35], [37], [38], [40]–[43], [45], [47], [51]–[53], [59], [61], [63], [68], [69], [74]–[76], [82], [83], [85], [87], [90], [91], [93]–[95], [97], [98], [101]
Small signal stability	[36], [47], [86]
Transient stability	[39], [78], [91], [93], [94], [101]
Voltage stability	[44], [50]–[52], [56], [60], [65], [75]
Security risk constraints	[102]
Environmental Related	
Constraints	References
Emission constraints	[82]

power flow equations are both non-linear and non-convex. AC power flow can be formulated in the polar form or rectangular form, as follows.

a: POLAR FORM

$$\begin{aligned}
 & \sum_{i \in N_{Gn}} P_{G,it} - \sum_{d \in N_{Ln}} P_{L,d,t} \\
 &= |V_{nt}| \sum_{m \in \Omega_n} |V_{mt}| * [G_{nm} * \cos \theta_{nm} + B_{nm} * \sin \theta_{nm}] \quad \forall n, \forall t \\
 &= \sum_{i \in N_{Gn}} Q_{G,it} - \sum_{d \in N_{Ln}} Q_{L,d,t} \\
 &|V_{nt}| \sum_{m \in \Omega_n} |V_{mt}| * [G_{nm} * \sin \theta_{nm} - B_{nm} * \cos \theta_{nm}] \quad \forall n, \forall t
 \end{aligned} \tag{62}$$

b: RECTANGULAR FORM

$$\begin{aligned}
 P_i &= \sum_{k=1}^N G_{ik}(E_i E_k + F_i F_k) + B_{ik}(F_i E_k + E_i F_k) \\
 Q_i &= \sum_{k=1}^N G_{ik}(F_i E_k + E_i F_k) - B_{ik}(E_i E_k + F_i F_k)
 \end{aligned} \tag{63}$$

In the rectangular form, bus voltages are represented by their real and imaginary components E and F rather than by magnitude and phase angle. The rectangular form has

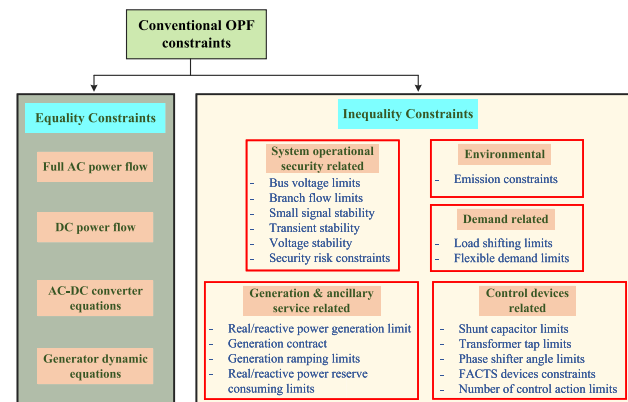


FIGURE 7. Categorization of conventional OPF constraints.

1) FULL AC POWER FLOW

The full version of the power flow equations is the alternating current (AC) power flow. OPF formulations incorporating AC

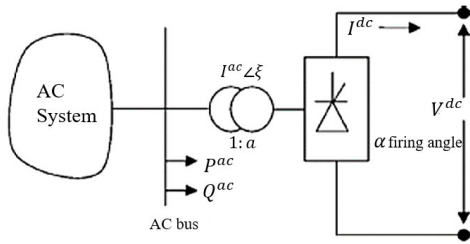


FIGURE 8. Equivalent circuit of DC terminal.

the advantage of eliminating trigonometric functions from the constraint set and of having constant second partial derivatives.

Loading parameter  $\lambda$  can also be included in the formulation to formulate the power flow equation at the critical point.

### 2) DC POWER FLOW

Direct current (DC) power flow extends the decoupling principle to form a linear power flow equation, by applying the following two assumptions: (1) the resistances in the transmission line are very small compared to the reactances and as thus neglected; (2) the differences between adjacent bus voltage angles are small. The formulation is as follows:

$$P_{G,n} - P_{L,n} = \sum_{m \in \Omega_n} |V_i| |V_k| B_{nm} (\delta_n - \delta_m) \quad \forall n \in N_B$$

$$Q_{G,n} - Q_{L,n} = \sum_{m \in \Omega_n} |V_i| |V_k| (-B_{nm}) \quad \forall n \in N_B \quad (64)$$

When only the real power flow is considered and all bus voltage magnitudes are approximated as 1.0, previous equations turn into fully linearized DC power flow equation:

$$P_{G,n} - P_{L,n} = \sum_{m \in \Omega_n} B_{nm} (\delta_n - \delta_m) \quad \forall n \in N_B \quad (65)$$

Both form of DC power flow equations neglect network losses, and inaccurately model or neglect the influence of reactive power. These can introduce unacceptable level of error in large power system models.

### 3) AC-DC CONVERTER EQUATIONS

The direct voltage and power at the converter are given by:

$$V^{dc} = aV^{ac} \cos \alpha - R_c I^{dc} \quad (66)$$

$$P^{dc} = V^{dc} I^{dc} \quad (67)$$

where

- $R_c$  is commutation resistance;
- $a$  is the transformer tap setting;
- $\alpha$  is the firing angle.

As shown in Fig. 8, neglecting the losses in the converter and its transformer and equating the expression for power on the AC and DC sides, the equation for power factor angle  $(\psi - \xi)$  is given by:

$$V^{dc} = aV^{ac} \cos(\psi - \xi) \quad (68)$$

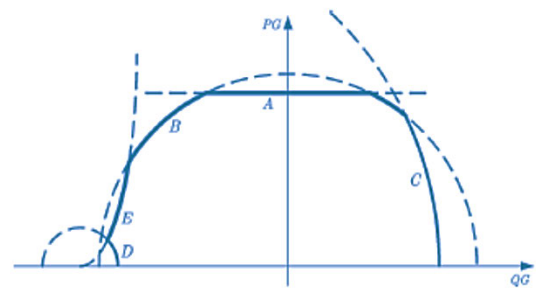


FIGURE 9. Generator capability curves.

and for the reactive power flowing from the AC bus into the converter terminal is

$$Q^{dc} = P^{ac} \tan(\psi - \xi) \quad (69)$$

where  $\psi$  is the alternating voltage angle and  $\xi$  is the alternating current angle.

### 4) GENERATOR DYNAMIC EQUATIONS

The classical generator model for transient stability analysis is adopted in the following formulation:

$$\dot{\delta}_i = \omega_i - \omega_0 \quad (70)$$

$$M_i \dot{\omega}_i = \omega_0 (-D_i \omega_i + P_{mi} - P_{ei}) \quad i \in N_G \quad (71)$$

$$P_{ei} = E_i'^2 G_{ii}' + \sum_{j=1, j \neq i}^{N_G} E_i' E_j' B_{ij}' \sin(\delta_i - \delta_j) + E_i' E_j' B G_{ij}' \cos(\delta_i - \delta_j) \quad (72)$$

where

- $\delta_i$  is rotor angle of  $i$ -th generator;
- $\omega_i$  is rotor speed of  $i$ -th generator;
- $\omega_0$  is rated rotor speed of generators;
- $M_i$  is the moment of inertia of  $i$ -th generator;
- $D_i$  is the damping constant of  $i$ -th generator;
- $P_{mi}$  is the mechanic power input of  $i$ -th generator;
- $P_{ei}$  is the electric power output of  $i$ -th generator;
- $E_i'$  is the internal voltage magnitude of the  $i$ -th generator;
- $G_{ij}' + jB_{ij}'$  is the transfer admittance between buses  $i$  and  $j$ .

### 5) REAL/REACTIVE POWER GENERATION LIMITS

Active/reactive power generation limits reflect the generator capacities, which mean that the active/reactive power output of each generator in the network is restricted by lower and upper limits as follows:

$$P_{G,i}^{\min} \leq P_{G,i} \leq P_{G,i}^{\max} \quad \forall i \in N_G$$

$$Q_{G,i}^{\min} \leq Q_{G,i} \leq Q_{G,i}^{\max} \quad \forall i \in N_G \quad (73)$$

The generator capacity curve is another way to describe the generation capacity of the generators:

Fig. 9 shows different generator capability curves in different zones. More specific expressions are shown below.

Zone A: Mechanical Source Limit:

$$P_G \leq P_{mec_{max}} \quad (74)$$

Zone B: Stator Current Limit:

$$P_G^2 + Q_G^2 = (V_t I_{a_{max}})^2 \quad (75)$$

Zone C: Over Excitation Limit:

$$P_G^2 + (Q_G + \frac{V_t^2}{X_q})^2 \leq (\frac{V_t E_{a_{max}}}{X_d} + V_t^2 (\frac{1}{X_q} - \frac{1}{X_d}) \cos(\delta - \theta))^2 \quad (76)$$

Zone D: Under Excitation Limit:

$$P_G^2 + (Q_G + \frac{V_t^2}{X_q})^2 \geq (\frac{V_t E_{a_{min}}}{X_d} + V_t^2 (\frac{1}{X_q} - \frac{1}{X_d}) \cos(\delta - \theta))^2 \quad (77)$$

Zone E: Stability Limit:

$$P_G^2 * (Q_G + \frac{V_t^2}{X_q}) \leq (Q_G + \frac{V_t^2}{X_q})^3 \quad (78)$$

where

- $P_{mec_{max}}$  is the maximum mechanical input;
- $V_t$  is the generator terminal voltage;
- $I_{a_{max}}$  is the maximum stator current;
- $X_q$  and  $X_p$  are sub-transient and synchronous reactance of generator, respectively;
- $E_{a_{max}}$  is the maximum stator voltage;
- $\delta$  and  $\theta$  are generator rotor angle and terminal voltage angle, respectively.

### 6) GENERATION CONTRACT

In a power market, generators may sign a contract to guarantee the amount of generation output for a time horizon:

$$CP_i^L \leq \sum_t P_{G,it} \leq CP_i^U \quad (79)$$

where  $CP_i^L$  and  $CP_i^U$  means the lower bound and upper bound of the available energy of unit  $i$  in the contact period.

In some cases, generators have fixed generation contract for the scheduling horizon:

$$\sum_t P_{G,it} = CP_i \quad (80)$$

where  $CP_i$  means the available energy of unit  $i$  in the contact period.

### 7) GENERATION RAMPING LIMITS

In the actual operating process of the generating unit, the operating range of all on-line units is restricted by their ramp rate limits. The inequality constraints due to the ramp limits are:

i) if power generation increases

$$P_{G,i} - P_{G,i}^0 \leq P_{UR,i} \Delta t, \quad \forall i \in N_G \quad (81)$$

ii) if power generation decreases

$$P_{G,i}^0 - P_{G,i} \leq P_{DR,i} \Delta t, \quad \forall i \in N_G \quad (82)$$

where  $P_{UR,i}$  (MW/h) is the up-ramp limit of the  $i$ -th generator; and  $P_{DR,i}$  (MW/h) is the down-ramp limit of the  $i$ -th generator.

### 8) REAL/REACTIVE POWER RESERVE CONSUMING LIMITS

In the operating stage, the usable reserve is limited by its pre-dispatched quantity. Example formulations are as follows.

$$\begin{aligned} -P_{R,i}^D &\leq \Delta P_{G,i} \leq P_{R,i}^U \\ -Q_{R,i}^D &\leq \Delta Q_{G,i} \leq Q_{R,i}^U \end{aligned} \quad (83)$$

where

- $P_{R,i}^D$  and  $P_{R,i}^U$  are the maximum downward and upward reserve of real power from unit  $i$ ;
- $\Delta P_{G,i}$  is the deployed reserve of real power by generating unit  $i$  in the operating condition;
- $Q_{R,i}^D$  and  $Q_{R,i}^U$  are the maximum downward and upward reserve of reactive power from unit  $i$ ;
- $\Delta Q_{G,i}$  is the deployed reserve of reactive power by generating unit  $i$  in the operating condition.

### 9) ANCILLARY RESERVE SCHEDULING REQUIREMENTS

The capacity reserve constraints are inequality constraints to ensure the right amount of capacity is procured according to the prescribed ancillary service requirements that are usually defined offline based on the load forecast and other operating system conditions. In the operational planning stage, the ancillary reserve capacity should be scheduled to fulfill the requirements, respecting the bid limits set by the bidders and the physical limits.

#### a: REGULATION UP REQUIREMENT

The following equation specifies the amount of reg-up that needs to be procured from generators in each region:

$$R_j^{RU} - \sum_{i \in I_{RU} \cap Z_j} RU_i \leq 0 \quad (84)$$

where

- $R_j^{RU}$ : requirement of reg-up in region;
- $Z_j$ : set of nodes in region.

#### b: SPINNING RESERVE REQUIREMENT

The total amount of reg-up and spin that needs to be procured from resources in each region is specified as

$$R_j^{RU} + R_j^{SP} - \sum_{i \in I_{RU} \cap Z_j} RU_i - \sum_{i \in I_{SP} \cap Z_j} SP_i \leq 0 \quad (85)$$

where  $R_j^{SP}$  denotes the requirement of spin in region.

*c: NON-SPINNING RESERVE REQUIREMENT*

The total amount of reg-up, spin, and non-spin that needs to be procured from resources in each region is specified as

$$R_j^{RU} + R_j^{SP} + R_j^{NS} - \sum_{i \in I_{RU} \cap Z_j} RU_i - \sum_{i \in I_{SP} \cap Z_j} SP_i - \sum_{i \in I_{NS} \cap Z_j} NS_i \leq 0 \quad (86)$$

where  $R_j^{NS}$  denotes the requirement of non-spin in region.

*d: REGULATION DOWN REQUIREMENT*

The amount of reg-down  $R_j^{RD}$  that needs to be procured from generators in each region is specified as

$$R_j^{RD} - \sum_{i \in I_{RD} \cap Z_j} RD_i \leq 0 \quad (87)$$

*e: REGULATION UP BID LIMIT*

The awarded quantity for reg-up for each generator must be nonnegative and may not be greater than an upper limit  $RU_i^{\max}$ , which represents the bid limit or physical limits such as ramp rates

$$0 \leq RU_i \leq RU_i^{\max} \quad (88)$$

*f: SPINNING BID LIMIT*

Similarly, the awarded quantity for spin is non-negative and limited by an upper limit  $SP_i^{\max}$  as follows:

$$0 \leq SP_i \leq SP_i^{\max} \quad (89)$$

*g: NON-SPINNING BID LIMIT*

The awarded quantity for non-spin is also non-negative and limited by an upper limit  $NS_i^{\max}$  as follows:

$$0 \leq NS_i \leq NS_i^{\max} \quad (90)$$

The non-spin bid quantity is a continuous variable from zero to the upper limit. However, if the resource is offline in real-time when the non-spin capacity is called upon to deliver energy, the resource will be dispatched to at least its minimum load according to the resource's energy bid in real time.

*h: REGULATION DOWN BID LIMIT*

The awarded quantity for reg-down is also non-negative and limited by an upper limit  $RD_i^{\max}$  as follows:

$$0 \leq RD_i \leq RD_i^{\max} \quad (91)$$

10) LOAD SHEDDING LIMITS

Load shedding quantity is restricted by the total load at the node, as well as the load shedding policy or agreement with costumers. Example formulation is as follows:

$$0 \leq L_d^{SH} \leq L_d^P \quad \forall d \in D \quad (92)$$

where

- $L_d^{SH}$  is the load shedding amount at load  $d$ ;
- $L_d^P$  is the real power demand at load  $d$ .

11) FLEXIBLE DEMAND LIMITS

Loads can be classified into constant power loads and dispatchable loads. The real power and reactive power of constant power loads are usually not controllable, except under load shedding. On the other hand, dispatchable loads or flexible loads are controllable, and they can be viewed as generators with negative power outputs. Example formulations are as follows:

$$\begin{aligned} P_{Li}^{\min} &\leq P_{Li} \leq P_{Li}^{\max} \\ Q_{Li}^{\min} &\leq Q_{Li} \leq Q_{Li}^{\max} \end{aligned} \quad (93)$$

where

- $P_{Li}^{\min}, P_{Li}, P_{Li}^{\max}$  are the minimum, dispatched and maximum real power demand dispatched at load  $i$ , respectively;
- $Q_{Li}^{\min}, Q_{Li}, Q_{Li}^{\max}$  are the minimum, dispatched and maximum reactive power demand dispatched at load  $i$ , respectively.

12) CONVENTIONAL CONTROL LIMITS (SHUNT CAPACITOR, TRANSFORMER, PHASE SHIFTER)

Control devices are constrained by their physical limits. Here are some examples: switchable shunt capacitors are restricted by their lower and upper reactive power limit, and transformer tap has maximum and minimum tap ratio. Their formulations are as follows.

*a: SHUNT CAPACITORS*

$$q_{ci-\min} \leq q_{ci} \leq q_{ci-\max} \quad i \in N_c \quad (94)$$

$$q_{ci} = q_{ci-\min} + N_{ci} * \Delta q_{ci} \quad (95)$$

*b: TRANSFORMER TAPPING*

$$T_{ci-\min} \leq T_{ci} \leq T_{ci-\max} \quad i \in N_T \quad (96)$$

$$T_{ci} = T_{ci-\min} + N_{Ti} * \Delta T_i \quad (97)$$

*c: TRANSFORMER TAPPING*

$$\phi^{\min} \leq \phi \leq \phi^{\max} \quad (98)$$

where

- $q_{ci-\min}, q_{ci}, q_{ci-\max}$  are the maximum, selected and minimum reactive power from shunt capacitor  $i$ , respectively;
- $N_{ci}, \Delta q_{ci}$  are number of steps and step size of shunt capacitor  $i$ , respectively;
- $T_{ci-\min}, T_{ci}, T_{ci-\max}$  are the maximum, selected and minimum tap ratio of transformer  $i$ , respectively;
- $N_{Ti}, \Delta T_i$  are number of steps and step size of transformer  $i$ , respectively;
- $\phi^{\min}, \phi, \phi^{\max}$  are the maximum, selected and minimum angle of phase shifter.

13) FACTS DEVICE LIMITS

Example formulation of FACTS constraints is as below:

#### a) TCSC CONTROLS (A KIND OF FACTS DEVICES)

$$x_{TCSC}^{\min} \leq x_{TCSC} \leq x_{TCSC}^{\max} \quad (99)$$

where  $x_{TCSC}$  is the control variable for TCSC,  $x_{TCSC}^{\min}$  and  $x_{TCSC}^{\max}$  are the minimum and maximum value of the control variable.

#### 14) NUMBER OF CONTROL ACTIONS LIMITS

Constraints for the number of control actions can be formulated with control variable status indicator  $s_i$ :

$$s_i(u_i^{\min} - u_i^0) \leq u_i - u_i^0 \leq s_i(u_i^{\max} - u_i^0) \quad i = 1, \dots, n$$

$$\sum_{i=1}^n s_i \leq N \quad s_i \in \{0, 1\} \quad i = 1, \dots, n \quad (100)$$

where  $s_i$  indicates the statuses of the corresponding control variable, with 1 meaning control actions and 0 meaning no action.

#### 15) BUS VOLTAGE LIMITS

Both the load and generation voltage buses are restricted by lower and upper limits as follows:

$$V_n^{\min} \leq V_n \leq V_n^{\max} \quad \forall n \quad (101)$$

There are also alternative formulations such as RMS voltage magnitude limit formulation as follows:

$$v^{\min} \leq \sqrt{|v_i^{(1)}|^2 + \sum_{h=2}^{h_{\max}} |v_i^{(h)}|^2} \leq v^{\max} \quad (102)$$

#### 16) BRANCH FLOW LIMITS

The power flow through transmission line must not exceed a maximum limit that is decided based on the characters of the line and the surrounding environment out of security consideration. Branch power flow of both directions should be limited.

$$-S_{nm}^{\max} \leq S_{nm} \leq S_{nm}^{\max} \quad \forall n, \forall m \in \Omega_n \quad (103)$$

where  $S_{nm}^{\max}$  is the maximum rating of transmission line connecting bus  $n$  and  $m$ .

#### 17) TRANSMISSION INTERFACE LIMITS

The power flow through each tie line or interface is constraint by its maximum and minimum capability:

$$-S_l^{\max} \leq S_l \leq S_l^{\max} \quad \forall l \in N_T, \forall t \quad (104)$$

where  $N_T$  is the set of tie lines,  $S_l^{\max}$  is the maximum power flow through the tie line  $l$ , and  $S_l$  is the power flow through tie line  $l$  at time  $t$ .

#### 18) SMALL SIGNAL STABILITY

According to the theory of small signal stability, the eigenvalues and eigenvectors of the system state matrix can reflect the stability of the system at the operating point and the characteristics of the oscillation. Particularly, a positive

real eigenvalue or real part of a complex pair of eigenvalues represents the small signal instability of test power system. The following equation denotes the small signal stability constraints.

$$\text{Re}(\lambda_i) < 0 \quad \forall i \in NE$$

$$\text{or } \text{Re}(\lambda_i) \leq \lambda_{\max} < 0 \quad (105)$$

where  $\text{Re}(\lambda_i)$  is the real part of the  $i$ -th eigenvalue, and  $\lambda_{\max}$  is the maximum allowed negative eigenvalue.

#### 19) TRANSIENT STABILITY

Generators angles with respect to the center of inertia (COI) are commonly used to indicate whether or not the system is stable when an explicit transient stability constraint is preferred. For a  $N_G$ -generator system with rotor angles  $\delta_i$  and inertia constant  $M_i$ , the position of COI is defined as

$$\delta_{COI} = \frac{\sum_{i=1}^{N_G} M_i \delta_i}{\sum_{i=1}^{N_G} M_i} \quad (106)$$

The inequality constraints of transient stability are formulated as

$$|\delta_i - \delta_{COI}|_{\max} \leq \delta_{\max} \quad (107)$$

where  $|\delta_i - \delta_{COI}|_{\max}$  corresponds to the maximum rotor angle deviation of  $i$ -th generator from COI, and  $\delta_{\max}$  is the maximum allowable rotor angle deviation. The setting of  $\delta_{\max}$  is often based on operation experience. Most utilities would have it set to  $100^\circ - 120^\circ$  to allow the system to have sufficient stability margin.

#### 20) VOLTAGE STABILITY

As discussed in 3.3.17, explicit voltage stability constraints are usually formulated based on indexes such as L-index or VCPI index. Example of voltage stability formulation using VCPI index is as follows:

$$VCPI_{\max} \leq VCPI_{\lim} \quad (108)$$

where  $VCPI_{\lim}$  is a desired threshold value to ensure a certain system security level and  $VCPI_{\max}$  is the maximum value of the VCPI index defined as

$$VCPI_{\max} = \max(VCPI_i), \quad i = 1, \dots, N_T \quad (109)$$

and  $N_T$  is the total number of lines in the system.

The maximum loading margin  $\lambda^*$  is constraint by:

$$\lambda^{\min} \leq \lambda^* \leq \lambda^{\max} \quad (110)$$

where  $\lambda$  is the parameter that drives the system to its maximum loading condition, and  $\lambda^*$  represents the maximum loading margin associated with the critical conditions.

21) SECURITY RISK CONSTRAINTS

Risk is a probabilistic index designed to reflect the overall stress of the system's operating condition under uncertainties. It extends from the notion of risk as an expected severity, i.e., the summation over possible contingency states of each state's probability multiplied by its severity. Risk indices can be calculated for severity capturing overload, cascading overload, low voltage, and voltage instability.

Taking the risk of post-contingency circuit overloading as an example, the system's overall risk can be expressed as:

$$Risk(g_1(P_0), \dots, g_{NC}(P_0)) = \sum_{k=1}^{NC} (Pr_k * Sev(g_k(P_0))) \tag{111}$$

where  $NC$  is the number of contingencies,  $Pr_k$  and  $Sev(\cdot)$  are occurrence probability and severity function for the  $k$ th contingency, respectively.  $P_0$  is the bus real power injection vector at normal state, and  $g_k(P_0)$  is the circuit power flow vector at the  $k$ -th contingency.

22) EMISSION CONSTRAINTS

The unit specific maximum hourly emission rate constraints at each generating unit may be represented as:

$$\sum_i e_i^n R_i \leq E_i^n + A_i^n \quad \forall n \in NA \tag{112}$$

where

- $e_i^n$  represents the emissions of pollutant  $n$  released per MWh from operation of generating unit at bus  $i$ ;
- $E_i^n$  represents the emissions constraint imposed by the appropriate regulatory authority;
- $A_i^n$  represents the quantity of any additional emissions allowance.

System-wide emission constraints designed to limit total annual emissions may be represented as:

$$\sum_i e_i^n R_i \leq E^n + A^n \quad \forall n \in NA \tag{113}$$

IV. SURVEY OF OPF FORMULATIONS WITH VARIABLE RENEWABLE ENERGY INTEGRATION

In this section, a survey of OPF objectives, control variables and constraints that are closely related to VRE integration is conducted. Summary tables and categorization graphs are provided, along with detailed formulations and explanations. literature-related OPF problem formulations considering VRE integration are surveyed.

A. VRE RELATED OBJECTIVE FUNCTIONS

Fig. 10 shows a categorization of the renewable-related objectives found in the literature. Table 10 summarizes the renewable-related objective found in the literature with references.

According to the categories from Fig. 6 and Table 7, the detailed mathematical formulas and explanations under each

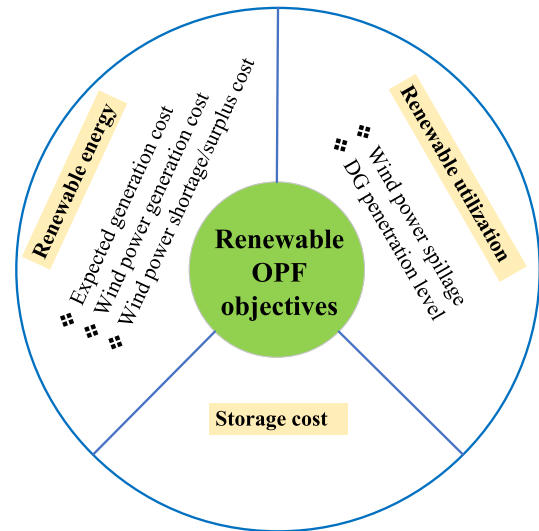


FIGURE 10. Categorization of VRE related OPF objectives.

TABLE 10. VRE related objective with references.

Variable Renewable Energy Related	
Objective	References
Expected generation cost	[100], [103]–[130]
Wind power generation cost	[45], [47], [47], [110], [111], [113]–[116], [119], [122], [123], [127], [129]–[136]
Wind power shortage/surplus cost	[47], [63], [118], [128], [131], [134], [135], [137]–[156]
Wind power spillage	[63], [103], [136], [157]–[192]
DG penetration level	[193]–[203]
Storage cost	[48], [109], [196], [204]–[209]

specific VRE related objective function are further given and shown as follows.

1) WIND POWER GENERATION COST

Wind energy comes for free, but electricity generation using wind is not free. Hardware and equipment cost money, as well as operating and maintaining the wind farms. Other than these, to deal with the variability of wind power, back up generation are needed, which brings extra costs.

$$C_W = \sum_{i=1}^{NW} a_i + b_i P_{Wi} \tag{114}$$

where

- $NW$  is the number of wind farms in the network;
- $a_i, b_i$  are the basic and linear cost coefficient of the  $i$ -th wind farm;
- $P_{Wi}$  is the real power output of the  $i$ -th wind farm.

### 2) WIND POWER SHORTAGE/SURPLUS COST

*Cost of Wind Power Shortage* can be defined as the cost generated by utilizing the system spinning reserve to deal with the situation in which the actual wind farm power output is lower than the scheduled power output. Followed is a possible formulation of this cost:

$$C_L = K_L \cdot Pr(P_{WF} < P_{schedule}) \times (P_{schedule} - E_{P_{WF} < P_{schedule}}(P_{WF})) \quad (115)$$

where

- $P_{schedule}$ ,  $P_{WF}$  are the scheduled and actual wind farm power outputs (in KW), respectively;
- $Pr(P_{WF} < P_{schedule})$  is the probability of wind power shortage occurrence;
- $E_{P_{WF} < P_{schedule}}(P_{WF})$  is the expectation of wind farm power output under  $P_{WF} < P_{schedule}$ ;
- $KL$  is a coefficient representing the adequacy of system spinning reserve and the difficulty to dispatch the spinning reserve (in \$/kWh).

*Cost of Wind Power Surplus* can be defined as the cost generated by the environmental benefit loss caused by decreasing wind farm power output. Followed is a possible formulation:

$$C_H = K_H \cdot Pr(P_{WF} > P_{schedule}) \times (E_{P_{WF} > P_{schedule}}(P_{WF}) - P_{schedule}) \quad (116)$$

where

- $P_{schedule}$ ,  $P_{WF}$  are the scheduled and actual wind farm power outputs (in KW), respectively;
- $Pr(P_{WF} > P_{schedule})$  is the probability of wind power surplus occurrence;
- $E_{P_{WF} > P_{schedule}}(P_{WF})$  is the expectation of wind farm power output under  $P_{WF} > P_{schedule}$ ;
- $KH$  is a coefficient representing the concerns for environment by local government (in \$/kWh).

### 3) WIND POWER SPILLAGE

Minimization of wind power production spillage or wind energy curtailment is an objective to maximize the usage of wind power generation. Wind power spillage can be formulated as below:

$$WS = \sum_{i=1}^{NW} W_{is}^{SP} \quad (117)$$

where

- $NW$  is the number of wind farms in the network;
- $W_{is}^{SP}$  is the wind power production spillage of wind farm  $i$  under the wind scenario  $s$ .

### 4) DG PENETRATION LEVEL

An example objective function to maximize the DG penetration level with respect to total system capacity, while DG only

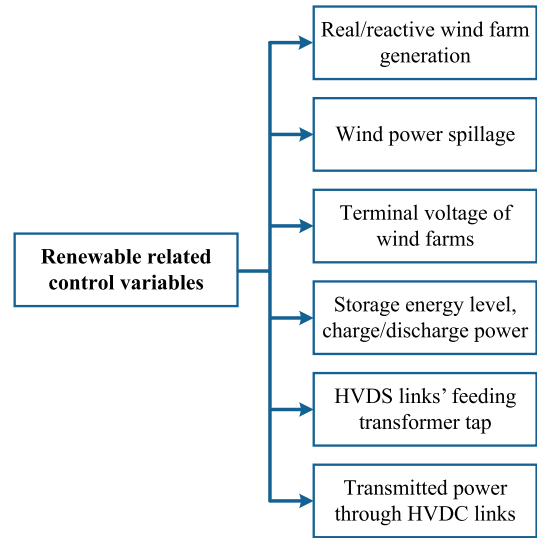


FIGURE 11. Categorization of VRE-related control variables.

delivering real power, can be defined as follows:

$$F(\%) = \frac{\sum_{i=1}^{N_{bus}} (P_{DG,i}^{inv} + P_{DG,i}^{syn})}{MVA_{Total}} \times 100 \quad (118)$$

where

- $P_{DG,i}^{inv}$ ,  $P_{DG,i}^{syn}$  are real power generation from inverter and synchronous based DG units, respectively;
- $MVA_{Total}$  is the total system MVA.

### 5) STORAGE COST

Storage related cost includes degradation costs associated with charging and discharging of storage device, and energy storage operation costs.

$$SC = \sum_{i \in N_s} \sum_{t \in T} [C_S * (P_{S,it}^d + P_{S,it}^c) + C_e * E_{S,it}] \quad (119)$$

where

- $N_s$  is set of storage devices;
- $C_s$  is the charging and discharging (degradation) cost of storage;
- $P_{S,it}^d$ ,  $P_{S,it}^c$  are the discharge and charge power of storage device, respectively;
- $C_e$  is the energy storage operation cost;
- $E_{S,it}$  is the energy level of storage device at time  $t$ .

### B. VRE RELATED CONTROL VARIABLES

Fig. 11 shows a categorization of the VRE-related control variables found in the literature. Table 11 summarizes the VRE-related control variables found in corresponding literature with references, and the control various types of being either continuous or discrete are considered as well.

TABLE 11. Categories of VRE-related control variables with references.

Variables	Type(s)	References
Real/ reactive wind farm generation	Continuous	[47], [55], [80], [122], [181], [206], [210]–[215]
Wind power spillage	Continuous	[63], [160], [161], [168]–[183], [186]–[190], [192]
Terminal voltage of wind farms	Continuous	[55], [214], [216]–[218]
Storage energy level, change and discharge power	Continuous	[48], [209], [219]–[221]
HVDC links' feeding transformer tap	Discrete	[55], [222]–[236]
Transmitted power through HVDC links	Continuous	[55], [237]–[252]

TABLE 12. VRE related constraints with references.

Variable Renewable Energy Related	
Constraints	References
HVDC power flow equations	[55], [72], [222]–[237], [253], [254]
Converter limits	[72], [226], [245], [255]–[263]
Grid code for wind farm connection	[72], [228], [239], [264]–[275]
Ancillary reserve requirements considering VREs	[31], [173], [276]–[282]
Storage constraints	[2], [17], [38], [48], [109], [176], [187], [208], [209], [219]–[221], [283]
Wind power generation limits	[47], [63], [105], [106], [108], [131], [284]
Renewable chance/risk constraints	[138], [174], [276], [285]–[292]

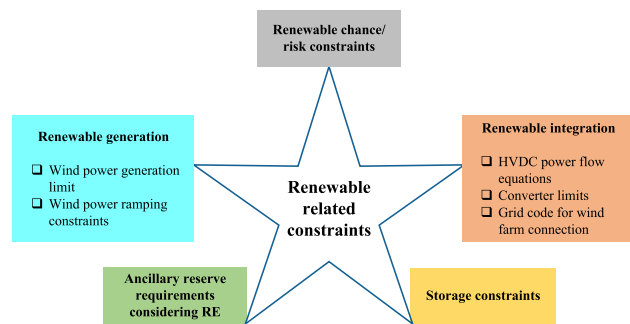


FIGURE 12. Categorization of VRE-related OPF constraints.

C. VRE RELATED CONSTRAINTS

Fig. 12 shows a categorization of the renewable-related constraints found in the literature. Table 12 summarizes the renewable-related constraints found in the literature with references.

According to the categories from Fig. 8 and Table 9, the detailed mathematical formulas and explanations under each specific VRE related constraint are further given and shown as follows.

1) HVDC POWER FLOW EQUATIONS

High-voltage direct current (HVDC) transmission lines can sometimes be a suitable choice for utilities to connect the off-shore wind farms or VREs in remote locations to the bulk transmission network. Different from the AC network, DC lines has different power flow equations, and should be formulated separately.

Following is an example of the power flow equations at the HVDC connected nodes, together with the connection diagram:

a: RECTIFIER SIDE

$$P_{d,r}(s, t) = P_{wg}(s, t) \tag{120}$$

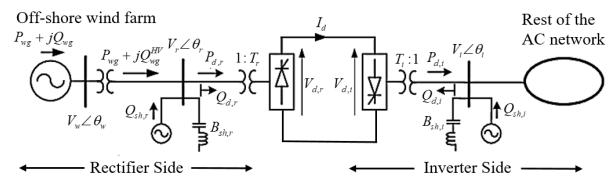


FIGURE 13. One-line diagram of the wind farm connection using the HVDC link.

$$Q_{d,r}(s, t) = Q_{wg}^{HV}(s, t) + B_{sh,r}V_r^2(s, t) + Q_{sh,r}(s, t) \tag{121}$$

b: INVERTER SIDE

$$P_i(s, t) = P_{Gi}(t) + P_{d,i}(s, t) - P_{Li}(t) \tag{122}$$

$$Q_i(s, t) = Q_i(t) + B_{Sh,i}V_i^2(s, t) - Q_{sh,i}(s, t) - Q_{d,i}(s, t) - Q_{Li}(t) \tag{123}$$

where

- $P_{Gi}(t)$ ,  $Q_{Gi}(t)$  are the active/reactive power generation by the thermal unit located in bus  $i$ ;
- $P_{d,i}$  is the active power flowing through the HVDC link  $i$ ;
- $P_{Li}(t)$ ,  $Q_{Li}(t)$  are the active/reactive load in bus  $i$ ;
- $B_{Sh,i}$  is the shunt admittance of passive filters at the ac side of HVDC terminal  $i$ ;
- $Q_{Sh,i}$  is the reactive power compensation at the ac side of HVDC terminal  $i$ ;
- $Q_{d,i}$  is the reactive power flowing into the ac side of the HVDC link  $i$ ;
- $P_{wg}$ ,  $Q_{wg}$  are the active/reactive power output of wind generator;
- $V_i$  is the voltage magnitude at bus  $i$ .

2) CONVERTER LIMITS

To ensure the safe operation of the converter, the steady state operating point must fulfill the PQ capacity limit. The

operating area of a VSC HVDC is limited by the following factors.

1) Constraint of IGBT Transistors Current:

$$-I_{cim\max} \leq I_{ci} \leq I_{cim\max} \quad (124)$$

where  $I_{cim\max}$  is the maximal current limit.

2) Constraint of Converter DC Voltage Level:

$$U_{dcimin} \leq U_{dci} \leq U_{dcimax} \quad (125)$$

where  $U_{dcimin}$ ,  $U_{dcimax}$  is the minimal and maximal limit of DC voltage, respectively.

3) Constraint of DC Cable Current:

$$-I_{dcmax} \leq I_{dcij} \leq I_{dcmax} \quad (126)$$

where

- $I_{dcij}$  is the current flow from DC bus  $i$  to  $j$ ;
- $I_{dcmax}$  is the current rating of the DC cable.

### 3) GRID CODE FOR WIND FARM CONNECTION

Transmission systems operators will supply a wind farm developer with a grid code to specify the requirements for interconnection to the transmission grid. The code usually specifies the requirements for power factor, frequency and low voltage ride through capability. The grid code is usually represented in the OPF as the following constraints of the reactive power:

$$Q_{scapi} \geq \alpha P_{si} \quad (127)$$

$$U_{simin} \leq U_{si} \leq U_{simax} \quad (128)$$

where

- $Q_{scapi} = \sqrt{S_{si}^2 - P_{si}^2}$  is the required reactive power capacity of the grid code;
- $S_{si}$  is the MVA rating of the  $i$ -th converter;
- $\alpha$  is calculated based on the power factor needed, e.g.,  $\alpha$  is 0.3287 if the power factor is chosen to be 0.95;
- $U_{si}$  is the AC voltage magnitude of the converter connected at PCC node;
- $U_{simax}$  and  $U_{simin}$  is the maximal and minimal limit of AC voltage defined by the grid code, respectively.

### 4) ANCILLARY RESERVE REQUIREMENTS CONSIDERING VRES

In order to control the impact of renewable energy uncertainty, more reserve is generally required. A formulation of reserve requirement considering renewable uncertainty is as below:

$$\sum_{n \in CG} RS_n + \sum_{n \in CG} RA_n \geq \alpha \cdot \sum_{n \in WG} E_n + \beta \cdot \sum_i PD_i \quad (129)$$

where

- $RS$ ,  $RA$  are vectors of spinning reserve and AGC reserve, respectively;
- $E$  is the vector of expected energy not served (EENS) by wind energy generation;
- $PD$  is the vector of real power demand;

-  $\alpha$ ,  $\beta$  are the rates of EENS and demand carried by reserves.

### 5) STORAGE CONSTRAINTS

The amount of energy storage at bus  $i$  is modeled as follows:

$$b_k(t+1) = b_k(t) + r_k(t)\Delta t, \quad \text{for } t = 1, \dots, T-1 \quad (130)$$

where  $b_k(t)$  denotes the amount of energy storage at time  $t$ , with initial condition  $b_k(1) = g_k \cdot r_k(t)$  is the rate of charge/discharge of energy at time  $t$ .

The amount of storage  $b_k(t)$  and charge/discharge rate  $r_k(t)$  are respectively bounded by:

$$0 \leq b_k(t) \leq B_k^{\max}, \quad \text{for } t \in T \quad (131)$$

$$R_k^{\min} \leq r_k(t) \leq R_k^{\max}, \quad \text{for } t \in 1, \dots, T-1 \quad (132)$$

The network constraint considering storage is formulated as:

$$V_k(t)I_k^*(t) = bP_k^g(t) - P_k^d(t) - r_k(t) + [Q_k^g(t) - Q_k^d(t) - s_k(t)]i \quad (133)$$

where  $s_k(t)$  is the reactive storage power inflow/outflow, which is bounded as:

$$s_k^{\min} \leq s_k(t) \leq s_k^{\max} \quad (134)$$

### 6) WIND POWER GENERATION LIMITS

Like thermal generators, wind power generation is also constrained by its maximum and minimum power generation. Example formulation is as follows:

$$0 \leq P_{W,w} \leq P_{W,w}^{\text{rate}} \quad \forall w \quad (135)$$

### 7) WIND POWER RAMPING CONSTRAINTS

The inter-temporal ramping constraint for the wind farm is given by

$$-WR_r \leq (P_{R,rt} - P_{R,r(t-1)}) \leq WR_r \quad \forall t, r \in N_G \quad (136)$$

### 8) RENEWABLE CHANCE/RISK CONSTRAINTS

Chance constraints are concerned of the possibilities that the up-ramp and down-ramp capability of the system will be sufficient to make up the differences between the predicted and actual available wind power generation. An example formulation is as below:

$$\Pr\left\{\sum_{i \in N_G} P_{u,i} \geq \sum_{j \in N_W} (P_{W,j} - P_{W,j}^{\text{av}})\right\} \geq c_u \quad (137)$$

$$\Pr\left\{\sum_{i \in N_G} P_{d,i} \geq \sum_{j \in N_W} (P_{W,j}^{\text{av}} - P_{W,j})\right\} \geq c_d \quad (138)$$

where  $c_u$ ,  $c_d$  are the confidence levels for having sufficient up and down regulation reserves.

These two constraints imply that the probabilities of having sufficient reserve capability should be greater than the confidence level of  $c_u$ ,  $c_d$ , respectively.

Chance constraint can also be used to represent the probability to effectively utilize renewable generation. The following chance constraint is associated with a risk level (e.g.,  $\varepsilon = 100\%$ ), which means the total utilization of wind power has to be larger than or equal to (e.g.,  $\beta = 85\%$ ) for at least  $100(1 - \varepsilon)$  percent of chance. The constraint can help utilities to comply with regulations which require a certain percentage of wind power utilization at a high probability.

$$\Pr(\beta \sum_{r \in N_R} PW(w_{rt}) \leq \sum_{r \in N_R} p_{R,rt}, \forall t) \geq 1 - \varepsilon \quad (139)$$

where  $p_{R,rt}$  is the wind power sold in real time market at time  $t$ .

## V. OPF IN DISTRIBUTION SYSTEMS WITH DERS

In this section, a brief survey of ACOPF in the distribution systems is provided. Electric power distribution networks are optimally designed to operate loads or equipment at rated systematic values (e.g., the voltage and thermal values). To protect this, power is required to be delivered at feasible voltages (i.e. within predetermined or acceptable lower and upper threshold limits of 0.95 p.u. and 1.05 p.u. in magnitude, respectively). To ensure these constraints are met, OPF analysis is a key part in distribution system operations.

However, distribution network control and management are becoming more complex. The increased connection of distributed energy sources (DERs) in networks creates additional technical challenges for distribution network operators [293], [294], [295]. The technical impacts associated with the penetration of DERs in distribution networks require detailed assessments of system patterns, making ACOPF analysis more important and challenging [296]. In addition, with increasing penetration of DERs in distribution networks, it is likely that voltage variability and in particular rapid voltage increases may occur at these locations, leading to issues of stability and reliability in the system.

As a result, we have reviewed papers within the past five years from these points of view, to summarize the current research stages and point out future research directions. The papers are reviewed through Web of Science with a focus on transmission system, distribution system, DERs, and the interface between transmission system operators (TSO) and distribution system operators (DSO). In summary, we have concluded 64 papers in Table 13. As more DERs, storage units and demand response programs have been integrated into the distribution systems, the adaptivity of the ACOPF analysis from these perspectives are aimed to be covered. As a result, Table 13 summarizes papers that have considered different aspects in the model including demand response, storage units, and renewable energy resources. To better analyze the integrated penetration level of DERs in the distribution system, the integration level of DERs that is over 50 % is reported in the table, along with different ways to analyze the intermittency of renewable energy resources by utilizing stochastic formulation. Another challenge arisen

from DERs and demand response program is the unbalanced three phases from the distribution system. Therefore, the formulation of ACOPF under unbalanced phases has been also reviewed as another factor in the table. An overview of the available test systems and practical systems have been also provided to encourage comparability of further research. Last but not the least, due to the proliferation of the DERs in distribution system, addressing OPF analysis requires paradigm shift in grid planning and operations, away from the current transmission-centralized approach to be inclusive for the increasingly coupled transmission and distribution systems. As a result, the OPF modeling of interface between TSO and DSO has been reviewed in the table as another essential factor.

As shown in Table 13, the majority of the papers considered one or more types of renewable energy sources and DERs in the distribution system. Despite of this, only 31 of the papers included storage units and 10 papers considered demand response programs, which are promising to more efficiently utilize the renewable energy resources. Compared to demand response programs, most of the storage unit modelings introduce linear constraints in solving the optimization problem, whereas the demand response programs involve more variations into the formulation and as a result, the nonlinearity can be potentially introduced to solve the problem.

Although most of the papers included renewable energy resources, 36 papers solved a deterministic problem, in other words, ignored the uncertain and intermittent characteristics of renewables. The integration levels of DERs are not clearly given in most of the papers even though the PV or wind turbine capacities are given in most of the papers. Nonetheless, the DERs scenarios are less in 50% in most of the papers based on rough estimations. To achieve the ambitious goal of 60-70% renewable integration in the next few decades, more attention should be paid to model the uncertainty in a higher level of DERs integration level.

As more DERs and storage units are integrated into the distribution system, it is likely to make three phases become more increasingly unbalanced. More specifically, variable single-phase DERs (e.g., solar PV) have the potential to increase the magnitude and variability of voltage unbalance in distribution system, potentially making conventional balanced phases approaches ineffective. Large unbalance reduces feeder power transfer capacity and increase system losses, and thus it is necessary to build comprehensive OPF formulation and modeling based on three-phased unbalanced distribution systems, especially with massive level of DER integration. As a matter of fact, there are only 4 out of the 64 papers that have considered the unbalanced structure of the system. References [297] and [298] considered the unbalanced formulation but it was not applied into the simulation case studies, and thus the convergence issues are not being tested.

To reduce the computational burden in weakly-meshed distribution systems with DERs, among 44 out of 64 papers,

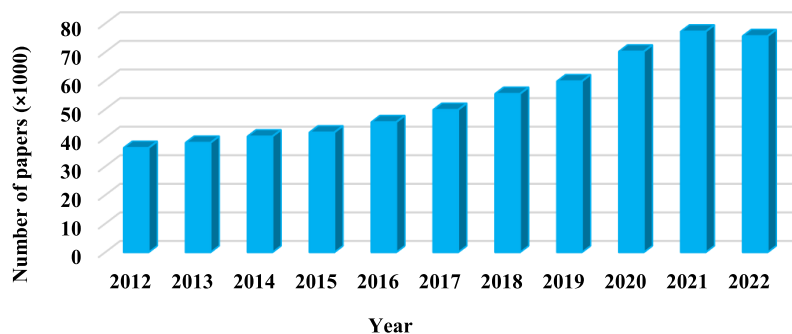


**FIGURE 14.** Number of papers published in the past 10 years that are related to optimal power flow modeling in distribution systems.

**TABLE 13.** ACOPF related system modeling in distribution system with references.

ACOPF Analysis in Distribution Systems	
Reviewed Perspectives	References
Demand Response	[128], [299]–[307]
Storage Units	[128], [299]–[303], [305], [306], [308]–[330]
DER Integration Level ( $\geq 50\%$ )	[309], [331], [332]
Stochastic Formulation	[290], [300], [302]–[304], [306]–[310], [313], [316], [319], [322], [326], [328], [330], [331], [333]–[343]
Unbalanced Phase Modeling	[312], [321], [332], [344]
Test System with Weakly-meshed Structures *	[128], [299], [303], [305], [306], [310], [313], [319], [325], [326], [330], [335], [339], [342], [345]–[350]
Practical Test System	[307], [312], [314], [318]–[320], [324], [329], [331], [333], [343], [346], [349], [351]
Interface between TSO and DSO	[128], [303], [319], [322], [323], [340], [343], [350], [351]

\* The complementary set of references are synthetic grids or IEEE standard cases.

the structure of the distribution systems was simplified to be radial-based, in which it is necessary to focus on weakly-meshed structured distribution system for further investigation. The practical test cases are wide spread around the world including but not limit to grids in China, Brazil, Italy, UK, US (Illinois), US (California) and Belgium (Flanders). As a result, more practical distribution data are required to better characterize the meshed structure and unbalanced phases for further research.

Based on the reviewed papers, by adding new technologies to power systems, such as smart grids, the conventional approaches can't meet the standards of now days power systems. Therefore new methodologies are needed to overcome this issue. Some of the gaps in this area are as follows that can also be considered as future directions:

- *Integration of Advanced Predictive Tools:* With the proliferation of renewable energy sources that have stochastic outputs, there's an increased need for predictive tools leveraging AI and machine learning for better

forecasting of renewable outputs, thereby enhancing the accuracy of OPF calculations.

- *Cyber-Physical Security in OPF:* The increasing digitalization in power systems, including smart grids, raises concerns about cyber-physical threats. Future OPF solutions must integrate security measures to ensure the reliable operation of power systems against malicious threats.
- *Decentralized and Distributed OPF:* With the rise of distributed energy resources (DERs) and microgrids, there's a growing need to develop decentralized OPF solutions that can cater to localized power generation and consumption patterns, ensuring optimal power flow at the community or even individual levels.
- *Grid-interactive Demand Response in OPF:* Future OPF solutions should incorporate more advanced demand response mechanisms, where consumers and utilities can interact in real-time to adjust power consumption based on grid conditions.
- *Adaptability to Grid Modernization:* Infrastructure enhancements, such as HVDC lines and FACTS devices, are shaping the modern power grid. OPF methodologies should evolve to cater to these advanced components for ensuring optimal power flow.
- *Regulatory and Policy Considerations:* As the power sector undergoes rapid transformations, the regulatory landscape is also changing. Future OPF solutions should be flexible enough to adapt to potential policy changes, especially regarding renewable integrations and emission targets.

## VI. CONCLUSION

Since the inception of OPF modeling in bulk power systems, the landscape of its applications has expanded and evolved significantly. The integration of variable renewable energy (VRE) sources and distributed energy resources (DERs) into power systems introduces a complex matrix of challenges and considerations. Foremost among these challenges is the need for greater operational flexibility. This flexibility is essential to balance the inherent unpredictability associated with renewable energy sources. Emphasizing this, there has

been a push towards leveraging fast-response controllable devices and storage solutions, enhancing network capacity utilization and overall system performance.

The rise of smart grids, with their distinctive features and capabilities, has rewritten many operational paradigms, including OPF. These grids offer a countermeasure to traditional OPF limitations, proposing innovative optimal operation schedules. The compelling benefits of integrating OPF into smart grids and renewable energy environments have garnered global interest from researchers and industry professionals. Through our survey, we ventured to present a comprehensive overview of various objective functions, decision variables, and network constraints. A key focus was to shed light on the integration of VREs into OPF. In parallel, we identified a range of under-researched areas, from phase topology in network distribution systems and demand response programs to the overarching question of how to maximize DER integration effectively.

In conclusion, while this research offers an in-depth look into conventional and VRE-integrated power systems, it's imperative to note that the OPF research landscape is vast and ever-evolving. The insights presented serve as a foundational guideline, aiming to equip researchers and enthusiasts with a holistic understanding of OPF's current state and potential trajectory.

## REFERENCES

- [1] J. Carpentier, "Contribution to the economic dispatch problem," *Bull. de la Societe Francoise des Electriciens*, vol. 3, no. 8, pp. 431–447, 1962.
- [2] M. B. Cain, R. P. O'Neill, and A. Castillo, "History of optimal power flow and formulations," *Federal Energy Regulatory Commission*, vol. 1, pp. 1–36, Dec. 2012.
- [3] B. H. Chowdhury and S. Rahman, "A review of recent advances in economic dispatch," *IEEE Trans. Power Syst.*, vol. 5, no. 4, pp. 1248–1259, Nov. 1990.
- [4] M. Huneault and F. D. Galiana, "A survey of the optimal power flow literature," *IEEE Trans. Power Syst.*, vol. 6, no. 2, pp. 762–770, May 1991.
- [5] J. A. Momoh, R. Adapa, and M. E. El-Hawary, "A review of selected optimal power flow literature to 1993. I. Nonlinear and quadratic programming approaches," *IEEE Trans. Power Syst.*, vol. 14, no. 1, pp. 96–104, Feb. 1999.
- [6] J. A. Momoh, M. E. El-Hawary, and R. Adapa, "A review of selected optimal power flow literature to 1993. II. Newton, linear programming and interior point methods," *IEEE Trans. Power Syst.*, vol. 14, no. 1, pp. 105–111, 1999.
- [7] W. Zhang, F. Li, and L. M. Tolbert, "Review of reactive power planning: Objectives, constraints, and algorithms," *IEEE Trans. Power Syst.*, vol. 22, no. 4, pp. 2177–2186, Nov. 2007.
- [8] W. Zhang and L. M. Tolbert, "Survey of reactive power planning methods," in *Proc. IEEE Power Eng. Soc. Gen. Meeting*, Jun. 2005, pp. 1430–1440.
- [9] K. Pandya, "A survey of optimal power flow method," *J. Theor. Appl. Inf. Technol.*, vol. 4, no. 5, pp. 450–458, 2008.
- [10] Z. Qiu, G. Deconinck, and R. Belmans, "A literature survey of optimal power flow problems in the electricity market context," in *Proc. IEEE/PES Power Syst. Conf. Expo.*, Mar. 2009, pp. 1–6.
- [11] X. Xia and A. M. Elaiw, "Optimal dynamic economic dispatch of generation: A review," *Electr. Power Syst. Res.*, vol. 80, no. 8, pp. 975–986, Aug. 2010.
- [12] S. Frank, I. Steponavice, and S. Rebennack, "Optimal power flow: A bibliographic survey I," *Energy Syst.*, vol. 3, no. 3, pp. 221–258, Sep. 2012.
- [13] S. Frank, I. Steponavice, and S. Rebennack, "Optimal power flow: A bibliographic survey II," *Energy Syst.*, vol. 3, no. 3, pp. 259–289, Sep. 2012.
- [14] D. Bienstock, "Progress on solving power flow problems," *Optima*, vol. 93, nos. 1–8, p. 1390, 2013.
- [15] S. Frank and S. Rebennack, "An introduction to optimal power flow: Theory, formulation, and examples," *IIE Trans.*, vol. 48, no. 12, pp. 1172–1197, Dec. 2016.
- [16] H. Abdi, S. D. Beigvand, and M. L. Scala, "A review of optimal power flow studies applied to smart grids and microgrids," *Renew. Sustain. Energy Rev.*, vol. 71, pp. 742–766, May 2017.
- [17] E. Mohagheghi, M. Alramlawi, A. Gabash, and P. Li, "A survey of real-time optimal power flow," *Energies*, vol. 11, no. 11, p. 3142, Nov. 2018.
- [18] F. Zohrizadeh, C. Josz, M. Jin, R. Madani, J. Lavaei, and S. Sojoudi, "A survey on conic relaxations of optimal power flow problem," *Eur. J. Oper. Res.*, vol. 287, no. 2, pp. 391–409, Dec. 2020.
- [19] R. P. O'Neill, T. Dautel, and E. Krall, "Recent ISO software enhancements and future software and modeling plans," Federal Energy Regulatory Commission, Washington, DC, USA, Tech. Rep., 2011.
- [20] Y.-Y. Hong and C.-M. Liao, "Short-term scheduling of reactive power controllers," *IEEE Trans. Power Syst.*, vol. 10, no. 2, pp. 860–868, May 1995.
- [21] J. A. Momoh, L. G. Dias, S. X. Guo, and R. Adapa, "Economic operation and planning of multi-area interconnected power systems," *IEEE Trans. Power Syst.*, vol. 10, no. 2, pp. 1044–1053, May 1995.
- [22] S. Majumdar, D. Chattopadhyay, and J. Parikh, "Interruptible load management using optimal power flow analysis," *IEEE Trans. Power Syst.*, vol. 11, no. 2, pp. 715–720, May 1996.
- [23] S. Y. Ge and T. S. Chung, "Optimal active power flow incorporating power flow control needs in flexible AC transmission systems," *IEEE Trans. Power Syst.*, vol. 14, no. 2, pp. 738–744, May 1999.
- [24] T. S. Chung, D. Qifeng, and Z. Boming, "Optimal active OPF with FACTS devices by an innovative load-equivalent approach," *IEEE Power Eng. Rev.*, vol. 20, no. 5, pp. 63–66, May 2000.
- [25] X. Wei, J. H. Chow, B. Fardanesh, and A.-A. Edrisft, "A common modeling framework of voltage-sourced converters for loadflow, sensitivity, and dispatch analysis," in *Proc. IEEE Power Eng. Soc. Gen. Meeting*, Jul. 2003, pp. 2569–2575.
- [26] W. Shao and V. Vittal, "LP-based OPF for corrective FACTS control to relieve overloads and voltage violations," *IEEE Trans. Power Syst.*, vol. 21, no. 4, pp. 1832–1839, Nov. 2006.
- [27] S. Salamat Sharif, J. H. Taylor, and E. F. Hill, "Dynamic online energy loss minimisation," *IEE Proc. Gener., Transmiss. Distrib.*, vol. 148, no. 2, p. 172, 2001.
- [28] W. D. Rosehart, C. A. Canizares, and V. H. Quintana, "Multiobjective optimal power flows to evaluate voltage security costs in power networks," *IEEE Trans. Power Syst.*, vol. 18, no. 2, pp. 578–587, May 2003.
- [29] D. Bhagwan Das and C. Patvardhan, "Useful multi-objective hybrid evolutionary approach to optimal power flow," *IEE Proc. Gener., Transmiss. Distrib.*, vol. 150, no. 3, p. 275, 2003.
- [30] A. J. Conejo, F. D. Galiana, J. M. Arroyo, R. Garcia-Bertrand, C. W. Chua, and M. Huneault, "Economic inefficiencies and cross-subsidies in an auction-based electricity pool," *IEEE Power Eng. Rev.*, vol. 22, no. 12, pp. 59–60, Feb. 2002.
- [31] T. Wu, M. Rothleder, Z. Alaywan, and A. D. Papalexopoulos, "Pricing energy and ancillary services in integrated market systems by an optimal power flow," *IEEE Trans. Power Syst.*, vol. 19, no. 1, pp. 339–347, Feb. 2004.
- [32] J. Hazra and A. K. Sinha, "Congestion management using multiobjective particle swarm optimization," *IEEE Trans. Power Syst.*, vol. 22, no. 4, pp. 1726–1734, Nov. 2007.
- [33] P. Wang, L. Goel, and Y. Ding, "Reliability assessment of restructured power systems using optimal load shedding technique," *IET Gener., Transmiss. Distrib.*, vol. 3, no. 7, pp. 628–640, Jul. 2009.
- [34] T. Niknam, M. R. Narimani, J. Aghaei, S. Tabatabaei, and M. Nayeripour, "Modified honey bee mating optimisation to solve dynamic optimal power flow considering generator constraints," *IET Gener., Transmiss. Distrib.*, vol. 5, no. 10, 2011.
- [35] T. Niknam, M. R. Narimani, J. Aghaei, and R. Azizipanah-Abarghooee, "Improved particle swarm optimisation for multi-objective optimal power flow considering the cost, loss, emission and voltage stability index," *IET Gener., Transmiss. Distrib.*, vol. 6, no. 6, pp. 515–527, 2012.

- [36] P. Li, H. Wei, B. Li, and Y. Yang, "Eigenvalue-optimisation-based optimal power flow with small-signal stability constraints," *IET Gener., Transmiss. Distrib.*, vol. 7, no. 5, pp. 440–450, May 2013.
- [37] M. Khanabadi, H. Ghasemi, and M. Doostizadeh, "Optimal transmission switching considering voltage security and N-1 contingency analysis," *IEEE Trans. Power Syst.*, vol. 28, no. 1, pp. 542–550, Feb. 2013.
- [38] D. Gayme and U. Topcu, "Optimal power flow with large-scale storage integration," *IEEE Trans. Power Syst.*, vol. 28, no. 2, pp. 709–717, May 2013.
- [39] X. Tu, L. Dessaint, and I. Kamwa, "A global approach to transient stability constrained optimal power flow using a machine detailed model," *Can. J. Electr. Comput. Eng.*, vol. 36, no. 1, pp. 32–41, Winter 2013.
- [40] C. Liu, J. Wang, Y. Fu, and V. Koritarov, "Multi-area optimal power flow with changeable transmission topology," *IET Gener., Transmiss. Distrib.*, vol. 8, no. 6, pp. 1082–1089, Jun. 2014.
- [41] R. Zhang, Z. Y. Dong, Y. Xu, K. P. Wong, and M. Lai, "Hybrid computation of corrective security-constrained optimal power flow problems," *IET Gener., Transmiss. Distrib.*, vol. 8, no. 6, pp. 995–1006, Jun. 2014.
- [42] A. Street, A. Moreira, and J. M. Arroyo, "Energy and reserve scheduling under a joint generation and transmission security criterion: An adjustable robust optimization approach," *IEEE Trans. Power Syst.*, vol. 29, no. 1, pp. 3–14, Jan. 2014.
- [43] W. Feng, L. A. Tuan, L. B. Tjernberg, A. Mannikoff, and A. Bergman, "A new approach for benefit evaluation of multiterminal VSC-HVDC using a proposed mixed AC/DC optimal power flow," *IEEE Trans. Power Del.*, vol. 29, no. 1, pp. 432–443, Feb. 2014.
- [44] T. Zabaoui, L. Dessaint, and I. Kamwa, "Preventive control approach for voltage stability improvement using voltage stability constrained optimal power flow based on static line voltage stability indices," *IET Gener., Transmiss. Distrib.*, vol. 8, no. 5, pp. 924–934, May 2014.
- [45] D. Thukaram and G. Yesuratnam, "Optimal reactive power dispatch in a large power system with AC-DC and facts controllers," *IET Gener., Transmiss. Distrib.*, vol. 2, no. 1, pp. 71–81, 2008.
- [46] R. A. Jabr, "Adjustable robust OPF with renewable energy sources," *IEEE Trans. Power Syst.*, vol. 28, no. 4, pp. 4742–4751, Nov. 2013.
- [47] L. Shi, C. Wang, L. Yao, Y. Ni, and M. Bazargan, "Optimal power flow solution incorporating wind power," *IEEE Syst. J.*, vol. 6, no. 2, pp. 233–241, Jun. 2012.
- [48] C. E. Murillo-Sánchez, R. D. Zimmerman, C. L. Anderson, and R. J. Thomas, "Secure planning and operations of systems with stochastic sources, energy storage, and active demand," *IEEE Trans. Smart Grid*, vol. 4, no. 4, pp. 2220–2229, Dec. 2013.
- [49] F. B. Alhasawi and J. V. Milanovic, "Techno-economic contribution of FACTS devices to the operation of power systems with high level of wind power integration," *IEEE Trans. Power Syst.*, vol. 27, no. 3, pp. 1414–1421, Aug. 2012.
- [50] F. Capitanescu and T. Van Cutsem, "Preventive control of voltage security margins: A multicontingency sensitivity-based approach," *IEEE Trans. Power Syst.*, vol. 17, no. 2, pp. 358–364, May 2002.
- [51] A. J. Conejo, F. Milano, and R. García-Bertrand, "Congestion management ensuring voltage stability," *IEEE Trans. Power Syst.*, vol. 21, no. 1, pp. 357–364, Feb. 2006.
- [52] A. Rabiee and M. Parniani, "Voltage security constrained multi-period optimal reactive power flow using benders and optimality condition decompositions," *IEEE Trans. Power Syst.*, vol. 28, no. 2, pp. 696–708, May 2013.
- [53] Y. Ding, M. Xie, Q. Wu, and J. Østergaard, "Development of energy and reserve pre-dispatch and re-dispatch models for real-time price risk and reliability assessment," *IET Gener., Transmiss. Distrib.*, vol. 8, no. 7, pp. 1338–1345, 2014.
- [54] P. J. Martínez-Lacañina, J. L. Martínez-Ramos, A. de la Villa-Jaén, and A. Marano-Marcolini, "Dc corrective optimal power flow based on generator and branch outages modelled as fictitious nodal injections," *IET Gener., Transmiss. Distrib.*, vol. 8, no. 3, pp. 401–409, 2013.
- [55] A. Rabiee and A. Soroudi, "Stochastic multiperiod OPF model of power systems with HVDC-connected intermittent wind power generation," *IEEE Trans. Power Del.*, vol. 29, no. 1, pp. 336–344, Feb. 2014.
- [56] X. Lin, A. K. David, and C. W. Yu, "Reactive power optimisation with voltage stability consideration in power market systems," *IEE Proc. Gener., Transmiss. Distrib.*, vol. 150, no. 3, p. 305, 2003.
- [57] M. De and S. K. Goswami, "Optimal reactive power procurement with voltage stability consideration in deregulated power system," *IEEE Trans. Power Syst.*, vol. 29, no. 5, pp. 2078–2086, Sep. 2014.
- [58] X. Wang, G. C. Ejebe, J. Tong, and J. G. Waight, "Preventive/corrective control for voltage stability using direct interior point method," *IEEE Trans. Power Syst.*, vol. 13, no. 3, pp. 878–883, Aug. 1998.
- [59] N. Martins, E. J. de Oliveira, W. C. Moreira, J. L. R. Pereira, and R. M. Fontoura, "Redispatch to reduce rotor shaft impacts upon transmission loop closure," *IEEE Trans. Power Syst.*, vol. 23, no. 2, pp. 592–600, May 2008.
- [60] F. Dong, B. H. Chowdhury, M. L. Crow, and L. Acar, "Improving voltage stability by reactive power reserve management," *IEEE Trans. Power Syst.*, vol. 20, no. 1, pp. 338–345, Feb. 2005.
- [61] F. Capitanescu, "Assessing reactive power reserves with respect to operating constraints and voltage stability," *IEEE Trans. Power Syst.*, vol. 26, no. 4, pp. 2224–2234, Nov. 2011.
- [62] J. C. O. Mello, A. C. G. Melo, and S. Granville, "Simultaneous transfer capability assessment by combining interior point methods and Monte Carlo simulation," *IEEE Trans. Power Syst.*, vol. 12, no. 2, pp. 736–742, May 1997.
- [63] A. Nasri, A. J. Conejo, S. J. Kazempour, and M. Ghandhari, "Minimizing wind power spillage using an OPF with FACTS devices," *IEEE Trans. Power Syst.*, vol. 29, no. 5, pp. 2150–2159, Sep. 2014.
- [64] L. Anh Tuan and K. Bhattacharya, "Competitive framework for procurement of interruptible load services," *IEEE Trans. Power Syst.*, vol. 18, no. 2, pp. 889–897, May 2003.
- [65] E. M. Viana, E. J. de Oliveira, N. Martins, J. L. R. Pereira, and L. W. de Oliveira, "An optimal power flow function to aid restoration studies of long transmission segments," *IEEE Trans. Power Syst.*, vol. 28, no. 1, pp. 121–129, Feb. 2013.
- [66] Y.-J. Zhang and Z. Ren, "Optimal reactive power dispatch considering costs of adjusting the control devices," *IEEE Trans. Power Syst.*, vol. 20, no. 3, pp. 1349–1356, Aug. 2005.
- [67] F. Capitanescu and L. Wehenkel, "Redispatching active and reactive powers using a limited number of control actions," *IEEE Trans. Power Syst.*, vol. 26, no. 3, pp. 1221–1230, Aug. 2011.
- [68] A. Marinakis, M. Glavic, and T. Van Cutsem, "Minimal reduction of unscheduled flows for security restoration: Application to phase shifter control," *IEEE Trans. Power Syst.*, vol. 25, no. 1, pp. 506–515, Feb. 2010.
- [69] F. Capitanescu and L. Wehenkel, "Computation of worst operation scenarios under uncertainty for static security management," *IEEE Trans. Power Syst.*, vol. 28, no. 2, pp. 1697–1705, May 2013.
- [70] B. Tamimi and S. Vaez-Zadeh, "An optimal pricing scheme in electricity markets considering voltage security cost," *IEEE Trans. Power Syst.*, vol. 23, no. 2, pp. 451–459, May 2008.
- [71] B. Cova, N. Losignore, P. Marannino, and M. Montagna, "Contingency constrained optimal reactive power flow procedures for voltage control in planning and operation," *IEEE Trans. Power Syst.*, vol. 10, no. 2, pp. 602–608, May 1995.
- [72] J. Cao, W. Du, H. F. Wang, and S. Q. Bu, "Minimization of transmission loss in meshed AC/DC grids with VSC-MTDC networks," *IEEE Trans. Power Syst.*, vol. 28, no. 3, pp. 3047–3055, Aug. 2013.
- [73] F. Xia and A. P. S. Meliopoulos, "A methodology for probabilistic simultaneous transfer capability analysis," *IEEE Trans. Power Syst.*, vol. 11, no. 3, pp. 1269–1278, Aug. 1996.
- [74] Y. Ou and C. Singh, "Assessment of available transfer capability and margins," *IEEE Power Eng. Rev.*, vol. 22, no. 5, p. 69, May 2002.
- [75] F. Milano, C. A. Canizares, and M. Invernizzi, "Multiobjective optimization for pricing system security in electricity markets," *IEEE Trans. Power Syst.*, vol. 18, no. 2, pp. 596–604, May 2003.
- [76] Y. Xiao, Y. H. Song, C.-C. Liu, and Y. Z. Sun, "Available transfer capability enhancement using facts devices," *IEEE Trans. Power Syst.*, vol. 18, no. 1, pp. 305–312, Feb. 2003.
- [77] W. Rosehart, C. Roman, and A. Schellenberg, "Optimal power flow with complementarity constraints," *IEEE Trans. Power Syst.*, vol. 20, no. 2, pp. 813–822, May 2005.
- [78] L. Hakim, J. Kubokawa, Y. Yuan, T. Mitani, Y. Zoka, N. Yorino, Y. Niwa, K. Shimomura, and A. Takeuchi, "A study on the effect of generation shedding to total transfer capability by means of transient stability constrained optimal power flow," *IEEE Trans. Power Syst.*, vol. 24, no. 1, pp. 347–355, Feb. 2009.

- [79] L. Gang, C. Jinfu, C. Defu, S. Dongyuan, and D. Xianzhong, "Probabilistic assessment of available transfer capability considering spatial correlation in wind power integrated system," *IET Gener., Transmiss. Distrib.*, vol. 7, no. 12, pp. 1527–1535, Dec. 2013.
- [80] H. Falaghi, M. Ramezani, C. Singh, and M.-R. Haghifam, "Probabilistic assessment of TTC in power systems including wind power generation," *IEEE Syst. J.*, vol. 6, no. 1, pp. 181–190, Mar. 2012.
- [81] P. Siano, C. Cecati, H. Yu, and J. Kolbusz, "Real time operation of smart grids via FCN networks and optimal power flow," *IEEE Trans. Ind. Inform.*, vol. 8, no. 4, pp. 944–952, Nov. 2012.
- [82] M. L. Baughman, S. N. Siddiqi, and J. W. Zarnikau, "Advanced pricing in electrical systems. I. Theory," *IEEE Trans. Power Syst.*, vol. 12, no. 1, pp. 489–495, Feb. 1997.
- [83] J. Young Choi, S.-H. Rim, and J.-K. Park, "Optimal real time pricing of real and reactive powers," *IEEE Trans. Power Syst.*, vol. 13, no. 4, pp. 1226–1231, Nov. 1998.
- [84] I. M. Nejdawi, K. A. Clements, L. M. Kimball, and P. W. Davis, "Nonlinear optimal power flow with intertemporal constraints," *IEEE Power Eng. Rev.*, vol. 20, no. 5, pp. 74–75, May 2000.
- [85] W. Urtubey and A. J. A. S. Costa, "Optimal power flow with intertemporal constraints as an aiding tool for demand-side management," *IEEE Proc. Gener., Transmiss. Distrib.*, vol. 149, no. 1, pp. 37–43, Jan. 2002.
- [86] J. Condren and T. W. Gedra, "Expected-security-cost optimal power flow with small-signal stability constraints," *IEEE Trans. Power Syst.*, vol. 21, no. 4, pp. 1736–1743, Nov. 2006.
- [87] J. Condren, T. W. Gedra, and P. Damrongkulkamjorn, "Optimal power flow with expected security costs," *IEEE Trans. Power Syst.*, vol. 21, no. 2, pp. 541–547, May 2006.
- [88] V. J. Gutierrez-Martinez, C. A. Cañizares, C. R. Fuerte-Esquivel, A. Pizano-Martinez, and X. Gu, "Neural-network security-boundary constrained optimal power flow," *IEEE Trans. Power Syst.*, vol. 26, no. 1, pp. 63–72, Feb. 2011.
- [89] A. Younesi, H. Shayeghi, P. Siano, and A. Safari, "A multi-objective resilience-economic stochastic scheduling method for microgrid," *Int. J. Electr. Power Energy Syst.*, vol. 131, Oct. 2021, Art. no. 106974. [Online]. Available: <https://www.sciencedirect.com/science/article/pii/S0142061521002143>
- [90] H. Wei, H. Sasaki, and J. Kubokawa, "A decoupled solution of hydro-thermal optimal power flow problem by means of interior point method and network programming," *IEEE Trans. Power Syst.*, vol. 13, no. 2, pp. 286–293, May 1998.
- [91] D. Gan, R. J. Thomas, and R. D. Zimmerman, "Stability-constrained optimal power flow," *IEEE Trans. Power Syst.*, vol. 15, no. 2, pp. 535–540, May 2000.
- [92] K. Xie and Y. H. Song, "Dynamic optimal power flow by interior point methods," *IEE Proc. Gener., Transmiss. Distrib.*, vol. 148, no. 1, p. 76, 2001.
- [93] Y. Yuan, J. Kubokawa, and H. Sasaki, "A solution of optimal power flow with multicontingency transient stability constraints," *IEEE Trans. Power Syst.*, vol. 18, no. 3, pp. 1094–1102, Aug. 2003.
- [94] N. Mo, Z. Y. Zou, K. W. Chan, and T. Y. G. Pong, "Transient stability constrained optimal power flow using particle swarm optimisation," *IET Gener., Transmiss. Distrib.*, vol. 1, no. 3, 2007.
- [95] R. Zárate-Miñano, A. J. Conejo, and F. Milano, "OPF-based security redispatching including FACTS devices," *IET Gener., Transmiss. Distrib.*, vol. 2, no. 6, 2008.
- [96] A. Pizano-Martinez, C. R. Fuerte-Esquivel, and D. Ruiz-Vega, "A new practical approach to transient stability-constrained optimal power flow," *IEEE Trans. Power Syst.*, vol. 26, no. 3, pp. 1686–1696, Aug. 2011.
- [97] F. Capitanescu, S. Fliscounakis, P. Panciatici, and L. Wehenkel, "Cautious operation planning under uncertainties," *IEEE Trans. Power Syst.*, vol. 27, no. 4, pp. 1859–1869, Nov. 2012.
- [98] Y. Nie, Z. Du, and J. Li, "AC–DC optimal reactive power flow model via predictor–corrector primal–dual interior–point method," *IET Gener., Transmiss. Distrib.*, vol. 7, no. 4, pp. 382–390, Apr. 2013.
- [99] S. Ahmed and G. Strbac, "A method for simulation and analysis of reactive power market," in *Proc. 21st Int. Conf. Power Ind. Comput. Appl. Connecting Utilities. PICA Millennium Beyond*, May 1999, pp. 337–342.
- [100] H. Song, B. Lee, S.-H. Kwon, and V. Ajjarapu, "Reactive reserve-based contingency constrained optimal power flow (RCCOPF) for enhancement of voltage stability margins," *IEEE Trans. Power Syst.*, vol. 18, no. 4, pp. 1538–1546, Nov. 2003.
- [101] Y. Sun, Y. Xinlin, and H. F. Wang, "Approach for optimal power flow with transient stability constraints," *IEE Proc. Gener., Transmiss. Distrib.*, vol. 151, no. 1, p. 8, 2004.
- [102] Q. Wang and J. D. McCalley, "Risk and 'N-1' criteria coordination for real-time operations," *IEEE Trans. Power Syst.*, vol. 28, no. 3, pp. 3505–3506, Aug. 2013.
- [103] X. Bai, L. Qu, and W. Qiao, "Robust AC optimal power flow for power networks with wind power generation," *IEEE Trans. Power Syst.*, vol. 31, no. 5, pp. 4163–4164, Sep. 2016.
- [104] D. Ke, C. Y. Chung, and Y. Sun, "A novel probabilistic optimal power flow model with uncertain wind power generation described by customized Gaussian mixture model," *IEEE Trans. Sustain. Energy*, vol. 7, no. 1, pp. 200–212, Jan. 2016.
- [105] R. Roy and H. T. Jadhav, "Optimal power flow solution of power system incorporating stochastic wind power using Gbest guided artificial bee colony algorithm," *Int. J. Electr. Power Energy Syst.*, vol. 64, pp. 562–578, Jan. 2015.
- [106] L. Roald, F. Oldewurtel, T. Krause, and G. Andersson, "Analytical reformulation of security constrained optimal power flow with probabilistic constraints," in *Proc. IEEE Grenoble Conf.*, Jun. 2013, pp. 1–6.
- [107] X. Fang, B.-M. Hodge, H. Jiang, and Y. Zhang, "Decentralized wind uncertainty management: Alternating direction method of multipliers based distributionally-robust chance constrained optimal power flow," *Appl. Energy*, vol. 239, pp. 938–947, Apr. 2019.
- [108] X. Fang, B.-M. Hodge, E. Du, N. Zhang, and F. Li, "Modelling wind power spatial–temporal correlation in multi-interval optimal power flow: A sparse correlation matrix approach," *Appl. Energy*, vol. 230, pp. 531–539, Nov. 2018.
- [109] K. M. Chandy, S. H. Low, U. Topcu, and H. Xu, "A simple optimal power flow model with energy storage," in *Proc. 49th IEEE Conf. Decis. Control (CDC)*, Dec. 2010, pp. 1051–1057.
- [110] Y. Z. Li and Q. H. Wu, "Downside risk constrained probabilistic optimal power flow with wind power integrated," *IEEE Trans. Power Syst.*, vol. 31, no. 2, pp. 1649–1650, Mar. 2016.
- [111] A. Attarha, N. Amjadi, and A. J. Conejo, "Adaptive robust AC optimal power flow considering load and wind power uncertainties," *Int. J. Electr. Power Energy Syst.*, vol. 96, pp. 132–142, Mar. 2018.
- [112] S. Shargh, B. K. Ghazani, B. Mohammadi-Ivatloo, H. Seyedi, and M. Abapour, "Probabilistic multi-objective optimal power flow considering correlated wind power and load uncertainties," *Renew. Energy*, vol. 94, pp. 10–21, Aug. 2016.
- [113] A. Gabash and P. Li, "Active-reactive optimal power flow in distribution networks with embedded generation and battery storage," *IEEE Trans. Power Syst.*, vol. 27, no. 4, pp. 2026–2035, Nov. 2012.
- [114] A. Panda and M. Tripathy, "Security constrained optimal power flow solution of wind-thermal generation system using modified bacteria foraging algorithm," *Energy*, vol. 93, pp. 816–827, Dec. 2015.
- [115] L. Xie, H.-D. Chiang, and S.-H. Li, "Optimal power flow calculation of power system with wind farms," in *Proc. IEEE Power Energy Soc. Gen. Meeting*, Jul. 2011, pp. 1–6.
- [116] L. Roald, G. Andersson, S. Misra, M. Chertkov, and S. Backhaus, "Optimal power flow with wind power control and limited expected risk of overloads," in *Proc. Power Syst. Comput. Conf. (PSCC)*, Jun. 2016, pp. 1–7.
- [117] S. Xia, X. Luo, K. W. Chan, M. Zhou, and G. Li, "Probabilistic transient stability constrained optimal power flow for power systems with multiple correlated uncertain wind generations," *IEEE Trans. Sustain. Energy*, vol. 7, no. 3, pp. 1133–1144, Jul. 2016.
- [118] Y. Zhang and G. B. Giannakis, "Robust optimal power flow with wind integration using conditional value-at-risk," in *Proc. IEEE Int. Conf. Smart Grid Commun. (SmartGridComm)*, Oct. 2013, pp. 654–659.
- [119] R. Azizpanah-Abarghoee, T. Niknam, M. Malekpour, F. Bavafa, and M. Kaji, "Optimal power flow based TU/CHP/PV/WPP coordination in view of wind speed, solar irradiance and load correlations," *Energy Convers. Manage.*, vol. 96, pp. 131–145, May 2015.
- [120] A. Arabali, M. Ghofrani, and M. Etezadi-Amoli, "Cost analysis of a power system using probabilistic optimal power flow with energy storage integration and wind generation," *Int. J. Electr. Power Energy Syst.*, vol. 53, pp. 832–841, Dec. 2013.
- [121] S. Rahmani and N. Amjadi, "A new optimal power flow approach for wind energy integrated power systems," *Energy*, vol. 134, pp. 349–359, Sep. 2017.

- [122] X. Fang, F. Li, Y. Wei, R. Azim, and Y. Xu, "Reactive power planning under high penetration of wind energy using benders decomposition," *IET Gener., Transmiss. Distrib.*, vol. 9, no. 14, pp. 1835–1844, Nov. 2015.
- [123] M. A. Abdulgalil, A. M. Amin, M. Khalid, and M. AlMuhaini, "Optimal sizing, allocation, dispatch and power flow of energy storage systems integrated with distributed generation units and a wind farm," in *Proc. IEEE PES Asia-Pacific Power Energy Eng. Conf. (APPEEC)*, Oct. 2018, pp. 680–684.
- [124] W. Bai, D. Lee, and K. Lee, "Stochastic dynamic optimal power flow integrated with wind energy using generalized dynamic factor model," *IFAC-PapersOnLine*, vol. 49, no. 27, pp. 129–134, 2016.
- [125] M. Fan, V. Vittal, G. T. Heydt, and R. Ayyanar, "Probabilistic power flow analysis with generation dispatch including photovoltaic resources," *IEEE Trans. Power Syst.*, vol. 28, no. 2, pp. 1797–1805, May 2013.
- [126] M. Sedghi, A. Ahmadian, and M. Aliakbar-Golkar, "Optimal storage planning in active distribution network considering uncertainty of wind power distributed generation," *IEEE Trans. Power Syst.*, vol. 31, no. 1, pp. 304–316, Jan. 2016.
- [127] H. T. Jadhav and R. Roy, "Stochastic optimal power flow incorporating offshore wind farm and electric vehicles," *Int. J. Electr. Power Energy Syst.*, vol. 69, pp. 173–187, Jul. 2015.
- [128] T. Soares, R. J. Bessa, P. Pinson, and H. Morais, "Active distribution grid management based on robust AC optimal power flow," *IEEE Trans. Smart Grid*, vol. 9, no. 6, pp. 6229–6241, Nov. 2018.
- [129] M. Ghofrani, A. Arabali, M. Etezadi-Amoli, and M. S. Fadali, "A framework for optimal placement of energy storage units within a power system with high wind penetration," *IEEE Trans. Sustain. Energy*, vol. 4, no. 2, pp. 434–442, Apr. 2013.
- [130] A. Panda, M. Tripathy, A. K. Barisal, and T. Prakash, "A modified bacteria foraging based optimal power flow framework for hydro-thermal-wind generation system in the presence of STATCOM," *Energy*, vol. 124, pp. 720–740, Apr. 2017.
- [131] R. A. Jabr and B. C. Pal, "Intermittent wind generation in optimal power flow dispatching," *IET Gener., Transmiss. Distrib.*, vol. 3, no. 1, pp. 66–74, Jan. 2009.
- [132] L. B. Shi, C. Wang, L. Z. Yao, L. M. Wang, Y. X. Ni, and B. Masoud, "Optimal power flow with consideration of wind generation cost," in *Proc. Int. Conf. Power Syst. Technol.*, Oct. 2010, pp. 1–5.
- [133] R. Kathiravan and R. P. K. Devi, "Optimal power flow model incorporating wind, solar, and bundled solar-thermal power in the restructured Indian power system," *Int. J. Green Energy*, vol. 14, no. 11, pp. 934–950, Sep. 2017.
- [134] C. Mishra, S. P. Singh, and J. Rokadia, "Optimal power flow in the presence of wind power using modified cuckoo search," *IET Gener., Transmiss. Distrib.*, vol. 9, no. 7, pp. 615–626, Apr. 2015.
- [135] A. Panda and M. Tripathy, "Optimal power flow solution of wind integrated power system using modified bacteria foraging algorithm," *Int. J. Electr. Power Energy Syst.*, vol. 54, pp. 306–314, Jan. 2014.
- [136] J. Cao, W. Du, and H. F. Wang, "Weather-based optimal power flow with wind farms integration," *IEEE Trans. Power Syst.*, vol. 31, no. 4, pp. 3073–3081, Jul. 2016.
- [137] S. Krohn, P.-E. Morthorst, and S. Awerbuch, "The economics of wind energy," *Eur. Wind Energy Assoc.*, vol. 3, pp. 28–29, Mar. 2009.
- [138] A. Sjodin, D. Gayme, and U. Topcu, "Risk-mitigated optimal power flow with high wind penetration," *Power*, vol. 14, no. 8, p. 15, 2012.
- [139] E. Rahimi, "Incorporating wind intermittency into probabilistic optimal power flow," *Int. J. Multidiscipl. Sci. Eng.*, vol. 4, no. 8, pp. 25–29, 2013.
- [140] J. Hetzer, D. C. Yu, and K. Bhattacharai, "An economic dispatch model incorporating wind power," *IEEE Trans. Energy Convers.*, vol. 23, no. 2, pp. 603–611, Jun. 2008.
- [141] B. Khan and P. Singh, "Optimal power flow techniques under characterization of conventional and renewable energy sources: A comprehensive analysis," *J. Eng.*, vol. 2017, pp. 1–16, Dec. 2017.
- [142] B. Sun, "Risk-averse design and operation of renewable energy power grids," Tech. Rep., 2015.
- [143] R. H. Wiser, A. Mills, J. Seel, T. Levin, and A. Botterud, "Impacts of variable renewable energy on bulk power system assets, pricing, and costs," Lawrence Berkeley Nat. Lab. (LBNL), Berkeley, CA, USA, Tech. Rep., 2017.
- [144] C. M. Grams, R. Beerli, S. Pfenninger, I. Staffell, and H. Wernli, "Balancing Europe's wind-power output through spatial deployment informed by weather regimes," *Nature Climate Change*, vol. 7, no. 8, pp. 557–562, Aug. 2017.
- [145] K. Teeparthi and D. M. Vinod Kumar, "Security-constrained optimal power flow with wind and thermal power generators using fuzzy adaptive artificial physics optimization algorithm," *Neural Comput. Appl.*, vol. 29, no. 3, pp. 855–871, Feb. 2018.
- [146] G. Hoste, M. Dvorak, and M. Z. Jacobson, "Matching hourly and peak demand by combining different renewable energy sources," Dept. Civil and Environ. Eng., Sanford Univ., Stanford, CA, USA, Tech. Rep., 2009.
- [147] I. U. Khan, N. Javaid, K. A. A. Gamage, C. J. Taylor, S. Baig, and X. Ma, "Heuristic algorithm based optimal power flow model incorporating stochastic renewable energy sources," *IEEE Access*, vol. 8, pp. 148622–148643, 2020.
- [148] K. Nakayama, C. Zhao, L. F. Bic, M. B. Dillencourt, and J. Brouwer, "Distributed real-time power flow control with renewable integration," in *Proc. IEEE Int. Conf. Smart Grid Commun. (SmartGridComm)*, Oct. 2013, pp. 516–521.
- [149] D. Phan and S. Ghosh, "Two-stage stochastic optimization for optimal power flow under renewable generation uncertainty," *ACM Trans. Model. Comput. Simul.*, vol. 24, no. 1, pp. 1–22, Jan. 2014.
- [150] O. Andrés-Martínez, L. F. Fuentes-Cortés, and A. Flores-Tlacuahuac, "110th anniversary: Modeling national power flow systems through the energy hub approach," *Ind. Eng. Chem. Res.*, vol. 58, no. 31, pp. 14252–14266, Aug. 2019.
- [151] P. Economics, "2017 state of the market report for the Ercot electricity markets," Tech. Rep., 2018.
- [152] Z. Wang, "On-line transient stability studies incorporating wind power," Tech. Rep., 2012.
- [153] F. Kunz, "Improving congestion management: How to facilitate the integration of renewable generation in Germany," *Energy J.*, vol. 34, no. 4, pp. 55–78, Oct. 2013.
- [154] L. Bajracharyay, S. Awasthi, S. Chalise, T. M. Hansen, and R. Tonkoski, "Economic analysis of a data center virtual power plant participating in demand response," in *Proc. IEEE Power Energy Soc. Gen. Meeting (PESGM)*, Jul. 2016, pp. 1–5.
- [155] Y. Gu, "Long-term power system capacity expansion planning considering reliability and economic criteria," Tech. Rep., 2011.
- [156] X. Fang, "Bi-level optimization considering uncertainties of wind power and demand response," Tech. Rep., 2016.
- [157] Y. Tang, Y. Liu, J. Ning, and J. Zhao, "Multi-time scale coordinated scheduling strategy with distributed power flow controllers for minimizing wind power spillage," *Energies*, vol. 10, no. 11, p. 1804, Nov. 2017.
- [158] P. Li, X. Guan, J. Wu, and X. Zhou, "Modeling dynamic spatial correlations of geographically distributed wind farms and constructing ellipsoidal uncertainty sets for optimization-based generation scheduling," *IEEE Trans. Sustain. Energy*, vol. 6, no. 4, pp. 1594–1605, Oct. 2015.
- [159] M. Doostizadeh, F. Aminifar, H. Ghasemi, and H. Lesani, "Energy and reserve scheduling under wind power uncertainty: An adjustable interval approach," *IEEE Trans. Smart Grid*, vol. 7, no. 6, pp. 2943–2952, Nov. 2016.
- [160] A. Kargarian, G. Hug, and J. Mohammadi, "A multi-time scale co-optimization method for sizing of energy storage and fast-ramping generation," *IEEE Trans. Sustain. Energy*, vol. 7, no. 4, pp. 1351–1361, Oct. 2016.
- [161] A. Nikoobakht, M. Mardaneh, J. Aghaei, V. Guerrero-Mestre, and J. Contreras, "Flexible power system operation accommodating uncertain wind power generation using transmission topology control: An improved linearised AC SCUC model," *IET Gener., Transmiss. Distrib.*, vol. 11, no. 1, pp. 142–153, Jan. 2017.
- [162] M. Liu, F. L. Quilumba, and W.-J. Lee, "Dispatch scheduling for a wind farm with hybrid energy storage based on wind and LMP forecasting," *IEEE Trans. Ind. Appl.*, vol. 51, no. 3, pp. 1970–1977, May 2015.
- [163] R. Yuan, J. Ye, J. Lei, and T. Li, "Integrated combined heat and power system dispatch considering electrical and thermal energy storage," *Energies*, vol. 9, no. 6, p. 474, Jun. 2016.
- [164] M. A. Hozouri, A. Abbaspour, M. Fotuhi-Firuzabad, and M. Moeini-Aghaie, "On the use of pumped storage for wind energy maximization in transmission-constrained power systems," *IEEE Trans. Power Syst.*, vol. 30, no. 2, pp. 1017–1025, Mar. 2015.
- [165] S. A. Pourmousavi, S. N. Patrick, and M. H. Nehrir, "Real-time demand response through aggregate electric water heaters for load shifting and balancing wind generation," *IEEE Trans. Smart Grid*, vol. 5, no. 2, pp. 769–778, Mar. 2014.

- [166] M. Ali, M. Z. Degefa, M. Humayun, A. Safdarian, and M. Lehtonen, "Increased utilization of wind generation by coordinating the demand response and real-time thermal rating," *IEEE Trans. Power Syst.*, vol. 31, no. 5, pp. 3737–3746, Sep. 2016.
- [167] A. Daraeipour, S. J. Kazempour, D. Patiño-Echeverri, and A. J. Conejo, "Strategic demand-side response to wind power integration," *IEEE Trans. Power Syst.*, vol. 31, no. 5, pp. 3495–3505, Sep. 2016.
- [168] S. Yang, D. Zeng, H. Ding, J. Yao, K. Wang, and Y. Li, "Multi-objective demand response model considering the probabilistic characteristic of price elastic load," *Energies*, vol. 9, no. 2, p. 80, Jan. 2016.
- [169] A. Kapetanaki, V. Levi, M. Buhari, and J. A. Schachter, "Maximization of wind energy utilization through corrective scheduling and FACTS deployment," *IEEE Trans. Power Syst.*, vol. 32, no. 6, pp. 4764–4773, Nov. 2017.
- [170] A. Elmitwally, A. Eladl, and J. Morrow, "Long-term economic model for allocation of FACTS devices in restructured power systems integrating wind generation," *IET Gener., Transmiss. Distrib.*, vol. 10, no. 1, pp. 19–30, Jan. 2016.
- [171] Y. Huo, P. Jiang, Y. Zhu, S. Feng, and X. Wu, "Optimal real-time scheduling of wind integrated power system presented with storage and wind forecast uncertainties," *Energies*, vol. 8, no. 2, pp. 1080–1100, Feb. 2015.
- [172] H.-I. Su and A. E. Gamal, "Modeling and analysis of the role of energy storage for renewable integration: Power balancing," *IEEE Trans. Power Syst.*, vol. 28, no. 4, pp. 4109–4117, Nov. 2013.
- [173] S. S. Reddy, "Multi-objective optimal power flow for a thermal-wind-solar power system," *J. Green Eng.*, vol. 7, no. 4, pp. 451–476, Apr. 2018.
- [174] D. Bienstock, M. Chertkov, and S. Harnett, "Chance-constrained optimal power flow: Risk-aware network control under uncertainty," *SIAM Rev.*, vol. 56, no. 3, pp. 461–495, Jan. 2014.
- [175] W. A. Bukhsh, C. Zhang, and P. Pinson, "An integrated multi-period OPF model with demand response and renewable generation uncertainty," *IEEE Trans. Smart Grid*, vol. 7, no. 3, pp. 1495–1503, May 2016.
- [176] A. Castillo and D. F. Gayme, "Evaluating the effects of real power losses in optimal power flow-based storage integration," *IEEE Trans. Control Netw. Syst.*, vol. 5, no. 3, pp. 1132–1145, Sep. 2018.
- [177] B. Deepthi and P. Suneetha, "Usage of OPF with facts devices to reduce wind power spillage," Tech. Rep., 2015.
- [178] M. Eslami Nia, M. Mohammadian, and M. H. Hemmatpour, "An approach for increasing wind power penetration in deregulated power system," *Scientia Iranica*, vol. 23, no. 3, pp. 1282–1293, Jul. 2016.
- [179] J. Li, F. Liu, Z. Li, C. Shao, and X. Liu, "Grid-side flexibility of power systems in integrating large-scale renewable generations: A critical review on concepts, formulations and solution approaches," *Renew. Sustain. Energy Rev.*, vol. 93, pp. 272–284, Oct. 2018.
- [180] K. Kim, F. Yang, V. M. Zavala, and A. A. Chien, "Data centers as dispatchable loads to harness stranded power," *IEEE Trans. Sustain. Energy*, vol. 8, no. 1, pp. 208–218, Jan. 2017.
- [181] M. Bavafa, "Optimal power flow considering voltage stability with significant wind penetration," Ph.D. dissertation, École de Technologie Supérieure, Montreal, QC, Canada, 2017.
- [182] A. Golshani, W. Sun, Q. Zhou, Q. P. Zheng, and Y. Hou, "Incorporating wind energy in power system restoration planning," *IEEE Trans. Smart Grid*, vol. 10, no. 1, pp. 16–28, Jan. 2019.
- [183] C. Ordoúdis, V. A. Nguyen, D. Kuhn, and P. Pinson, "Energy and reserve dispatch with distributionally robust joint chance constraints," Tech. Rep., 2018. [Online]. Available: <http://www.optimization-online.org>
- [184] *EWEA Position Paper on Priority Dispatch of Wind Power*, EWEA, European Wind Energy Association, Brussels, Belgium, 2014.
- [185] K. Neuhoff, J. Barquin, J. W. Bialek, R. Boyd, C. J. Dent, F. Echavarren, T. Grau, C. von Hirschhausen, B. F. Hobbs, F. Kunz, C. Nabe, G. Papaefthymiou, C. Weber, and H. Weigt, "Renewable electric energy integration: Quantifying the value of design of markets for international transmission capacity," *Energy Econ.*, vol. 40, pp. 760–772, Nov. 2013.
- [186] E. Nycander, L. Söder, R. Eriksson, and C. Hamon, "Minimising wind power curtailments using OPF considering voltage stability," *J. Eng.*, vol. 2019, no. 18, pp. 5064–5068, Jul. 2019.
- [187] S. S. Reddy, "Optimal scheduling of thermal-wind-solar power system with storage," *Renew. Energy*, vol. 101, pp. 1357–1368, Feb. 2017.
- [188] J. F. Marley, D. K. Molzahn, and I. A. Hiskens, "Solving multiperiod OPF problems using an AC-QP algorithm initialized with an SOCP relaxation," *IEEE Trans. Power Syst.*, vol. 32, no. 5, pp. 3538–3548, Sep. 2017.
- [189] A. Hamann and G. Hug, "Integrating variable wind power using a hydropower cascade," *Energy Proc.*, vol. 87, pp. 108–115, Jan. 2016.
- [190] S. Abedi, M. He, and D. Obadina, "Congestion risk-aware unit commitment with significant wind power generation," *IEEE Trans. Power Syst.*, vol. 33, no. 6, pp. 6861–6869, Nov. 2018.
- [191] R. Fernández-Blanco, Y. Dvorkin, B. Xu, Y. Wang, and D. S. Kirschen, "Energy storage siting and sizing in the WECC area and the CAISO system," Tech. Rep., 2016.
- [192] H. Bitaraf and S. Rahman, "Optimal operation of energy storage to minimize wind spillage and mitigate wind power forecast errors," in *Proc. IEEE Power Energy Soc. Gen. Meeting (PESGM)*, Jul. 2016, pp. 1–5.
- [193] A. Martínez-Mares and C. R. Fuente-Esquivel, "A robust optimization approach for the interdependency analysis of integrated energy systems considering wind power uncertainty," *IEEE Trans. Power Syst.*, vol. 28, no. 4, pp. 3964–3976, Nov. 2013.
- [194] J. Radosavljevic, M. Jevtic, D. Klimenta, and N. Arsic, "Optimal power flow for distribution networks with distributed generation," *Serbian J. Electr. Eng.*, vol. 12, no. 2, pp. 145–170, 2015.
- [195] L. F. Ochoa and G. P. Harrison, "Using AC optimal power flow for DG planning and optimisation," in *Proc. IEEE PES Gen. Meeting*, Jul. 2010, pp. 1–7.
- [196] F. Meng, "A generalized optimal power flow program for distribution system analysis and operation with distributed energy resources and solid state transformers," Tech. Rep., 2014.
- [197] V. R. Pandi, H. H. Zeineldin, W. Xiao, and A. F. Zobaa, "Optimal penetration levels for inverter-based distributed generation considering harmonic limits," *Electr. Power Syst. Res.*, vol. 97, pp. 68–75, Apr. 2013.
- [198] K. Gnanambal and S. Suriya, "Optimal sizing of distributed generation for voltage profile improvement considering maximum loadability limit," *Int. J. Innov. Res. Sci., Eng. Technol.*, vol. 3, no. 3, pp. 304–309, 2014.
- [199] M. Naghdi, M.-A. Shafiyi, and M.-R. Haghifam, "A combined probabilistic modeling of renewable generation and system load types to determine allowable DG penetration level in distribution networks," *Int. Trans. Electr. Energy Syst.*, vol. 29, no. 1, Jan. 2019, Art. no. e2696.
- [200] K. Khalilnejad, "Multi-objective optimal battery placement in distribution networks," Tech. Rep., 2018.
- [201] R. Dobbe, O. Sondermeijer, D. Fridovich-Keil, D. Arnold, D. Callaway, and C. Tomlin, "Toward distributed energy services: Decentralizing optimal power flow with machine learning," *IEEE Trans. Smart Grid*, vol. 11, no. 2, pp. 1296–1306, Mar. 2020.
- [202] P. Sudhakar and C. Rambabu, "DG placement and penetration under standard market design using ga and PSO," Tech. Rep.
- [203] C. Mendoza, "Optimal allocation of energy storage and wind generation in power distribution systems," Tech. Rep., 2019.
- [204] J. Chengquan and W. Peng, "Dynamic optimal power flow including energy storage with adaptive operation costs," in *Proc. IECN 41st Annu. Conf. IEEE Ind. Electron. Soc.*, Nov. 2015, pp. 1561–1566.
- [205] Z. Hu and W. T. Jewell, "Optimal power flow analysis of energy storage for congestion relief, emissions reduction, and cost savings," in *Proc. IEEE/PES Power Syst. Conf. Expo.*, Mar. 2011, pp. 1–8.
- [206] D. Gayme and U. Topcu, "Optimal power flow with distributed energy storage dynamics," in *Proc. Amer. Control Conf.*, Jun. 2011, pp. 1536–1542.
- [207] J. F. Marley and I. A. Hiskens, "Multi-period AC-QP optimal power flow including storage," in *Proc. Power Syst. Comput. Conf. (PSCC)*, Jun. 2016, pp. 1–7.
- [208] P. Fortenbacher, M. Zellner, and G. Andersson, "Optimal sizing and placement of distributed storage in low voltage networks," in *Proc. Power Syst. Comput. Conf. (PSCC)*, Jun. 2016, pp. 1–7.
- [209] A. M. Alzahrani, "Convex optimization approach to the optimal power flow problem in DC-microgrids with energy storage," Tech. Rep., 2018.
- [210] J. L. Rodríguez-Amenedo, S. Arnalte, and J. C. Burgos, "Automatic generation control of a wind farm with variable speed wind turbines," *IEEE Power Eng. Rev.*, vol. 22, no. 5, p. 65, May 2002.
- [211] D. F. Opila, A. M. Zeynu, and I. A. Hiskens, "Wind farm reactive support and voltage control," in *Proc. IREP Symp. Bulk Power Syst. Dyn. Control VIII (IREP)*, Aug. 2010, pp. 1–10.

- [212] J. Aho, A. Buckspan, J. Laks, P. Fleming, Y. Jeong, F. Dunne, M. Churchfield, L. Pao, and K. Johnson, "A tutorial of wind turbine control for supporting grid frequency through active power control," in *Proc. Amer. Control Conf. (ACC)*, Jun. 2012, pp. 3120–3131.
- [213] S. Duman, J. Li, L. Wu, and U. Gucenc, "Optimal power flow with stochastic wind power and FACTS devices: A modified hybrid PSO-GSA with chaotic maps approach," *Neural Comput. Appl.*, vol. 32, no. 12, pp. 8463–8492, Jun. 2020.
- [214] J. A. Kline, "Centralized wind power plant voltage control with optimal power flow algorithm," Tech. Rep., 2011.
- [215] A. Gabash and P. Li, "On variable reverse power flow—Part I: Active-reactive optimal power flow with reactive power of wind stations," *Energies*, vol. 9, no. 3, p. 121, Feb. 2016.
- [216] M. J. Carrizosa, F. D. Navas, G. Damm, and F. Lamnabhi-Lagarriague, "Optimal power flow in multi-terminal HVDC grids with offshore wind farms and storage devices," *Int. J. Electr. Power Energy Syst.*, vol. 65, pp. 291–298, Feb. 2015.
- [217] R. Keypour, A. A. Rashidi, and M. Jazaeri, "Probabilistic voltage stability constrained optimal power flow considering wind farms," in *Proc. IEEE Region 8 Int. Conf. Comput. Technol. Electr. Electron. Eng. (SIBIRCON)*, Jul. 2010, pp. 533–538.
- [218] Y. Zhou, L. Zhao, W.-J. Lee, Z. Zhang, and P. Wang, "Optimal power flow in hybrid AC and multi-terminal HVDC networks with offshore wind farm integration based on semidefinite programming," in *Proc. IEEE Innov. Smart Grid Technol.-Asia (ISGT Asia)*, May 2019, pp. 207–212.
- [219] A. Maffei, D. Meola, G. Marafioti, G. Palmieri, L. Iannelli, G. Mathisen, E. Bjerkan, and L. Glielmo, "Optimal power flow model with energy storage, an extension towards large integration of renewable energy sources," *IFAC Proc. Volumes*, vol. 47, no. 3, pp. 9456–9461, 2014.
- [220] K. Baker, J. Guo, G. Hug, and X. Li, "Distributed MPC for efficient coordination of storage and renewable energy sources across control areas," *IEEE Trans. Smart Grid*, vol. 7, no. 2, pp. 992–1001, Mar. 2016.
- [221] Z. Wang, J. Zhong, D. Chen, Y. Lu, and K. Men, "A multi-period optimal power flow model including battery energy storage," in *Proc. IEEE Power Energy Soc. Gen. Meeting*, Jul. 2013, pp. 1–5.
- [222] D. Jovicic and B. T. Ooi, "Tapping on HVDC lines using DC transformers," *Electr. Power Syst. Res.*, vol. 81, no. 2, pp. 561–569, Feb. 2011.
- [223] U. Bondhala and V. Sarkar, "Power flow studies of an AC–DC transmission system," Ph.D. dissertation, Indian Inst. Technol. Hyderabad, Hyderabad, India, 2011.
- [224] S. M. Amrr, M. S. J. Asghar, I. Ashraf, and M. Meraj, "A comprehensive review of power flow controllers in interconnected power system networks," *IEEE Access*, vol. 8, pp. 18036–18063, 2020.
- [225] L.-e. Juhlin, "Power flow control in a meshed HVDC power transmission network," U.S. Patent 8 847 430, Sep. 30, 2014.
- [226] M. Baradar, "Modeling of multi terminal HVDC systems in power flow and optimal power flow formulations," Ph.D. dissertation, KTH Royal Inst. Technol., Stockholm, Sweden, 2013.
- [227] B. Kazemtabrizi, "Mathematical modelling of multi-terminal VSC-HVDC links in power systems using optimal power flows," Ph.D. dissertation, Univ. Glasgow, Glasgow, Scotland, 2011.
- [228] D. Dhua, S. Huang, and Q. Wu, "Optimal power flow modelling and analysis of hybrid AC–DC grids with offshore wind power plant," *Energy Proc.*, vol. 141, pp. 572–579, Dec. 2017.
- [229] M. Imhof, "Voltage source converter based HVDC-modelling and coordinated control to enhance power system stability," Ph.D. dissertation, ETH Zürich, Zürich, Switzerland, 2015.
- [230] M. Kirik, "VSC-HVDC for long-term voltage stability improvement," Ph.D. dissertation, Citeseer, Princeton, NJ, USA, 2009.
- [231] J. Pan, R. Nuqui, L. Tang, and P. Holmberg, "VSC-HVDC control and application in meshed ac networks," in *Proc. IEEE Power Eng. Soc. Gen. Meeting*, Jul. 2008, pp. 20–24.
- [232] L. M. C. Gonzalez, "Modelling of multi-terminal VSC-HVDC links for power flows and dynamic simulations of AC/DC power networks," Tech. Rep., 2016.
- [233] A. Rabiee, A. Soroudi, and A. Keane, "Information gap decision theory based OPF with HVDC connected wind farms," *IEEE Trans. Power Syst.*, vol. 30, no. 6, pp. 3396–3406, Nov. 2015.
- [234] X. Wang, "Coordination of power flow control by using facts device and HVD transmission system," Ph.D. dissertation, Cardiff Univ., Cardiff, Wales, 2016.
- [235] S. Henry, O. Despouys, R. Adapa, C. Barthold, K. Bell, J. Binard, A. Edris, P. Egrot, W. Hung, and G. Irwin, *Influence of Embedded HVDC Transmission on System Security and AC Network Performance*. Paris, France: Cigré, 2013.
- [236] E. Acha and B. Kazemtabrizi, "A new STATCOM model for power flows using the Newton–Raphson method," *IEEE Trans. Power Syst.*, vol. 28, no. 3, pp. 2455–2465, Aug. 2013.
- [237] A. Rabiee and A. Soroudi, "Multi-period OPF model of power systems with HVDC connected intermittent wind power generation," Tech. Rep.
- [238] M. Giuntoli and S. Schmitt, "Security analysis of embedded HVDC in transmission grids," in *Proc. Int. Symp. Energy Syst. Optim. Cham*, Switzerland: Birkhäuser, 2018, pp. 13–25.
- [239] M. E. Montilla-DJesus, S. Arnaltes, E. D. Castronuovo, and D. Santos-Martin, "Optimal power transmission of offshore wind power using a VSC-HVdc interconnection," *Energies*, vol. 10, no. 7, p. 1046, Jul. 2017.
- [240] A. Raza, A. Mustafa, K. Rouzbehi, M. Jamil, S. O. Gilani, G. Abbas, U. Farooq, and M. N. Shehzad, "Optimal power flow and unified control strategy for multi-terminal HVDC systems," *IEEE Access*, vol. 7, pp. 92642–92650, 2019.
- [241] S. Sayah and A. Hamouda, "Optimal power flow solution of integrated AC–DC power system using enhanced differential evolution algorithm," *Int. Trans. Electr. Energy Syst.*, vol. 29, no. 2, Feb. 2019, Art. no. e2737.
- [242] M. P. Musau, A. N. Odero, C. W. Wekesa, and N. Angela, "Economic dispatch for HVDC bipolar system with HVAC and optimal power flow comparisons using improved genetic algorithm (IGA)," *Int. J. Eng. Res. Technol. (IJERT)*, vol. 4, no. 8, pp. 790–799, 2015.
- [243] M. A. Djehaf, Z. S. Ahmed, and Y. D. Kobibi, "AC versus DC link comparison based on power flow analysis of a multimachine power system," *Leonardo J. Sci.*, vol. 13, no. 24, pp. 1–14, 2014.
- [244] S. Khan and S. Bhowmick, "Effect of DC link control strategies on multiterminal AC–DC power flow," *Adv. Electr. Eng.*, vol. 2015, pp. 1–15, Apr. 2015.
- [245] M. Aragüés-Peñalba, A. E. Alvarez, S. G. Arellano, and O. Gomis-Bellmunt, "Optimal power flow tool for mixed high-voltage alternating current and high-voltage direct current systems for grid integration of large wind power plants," *IET Renew. Power Gener.*, vol. 9, no. 8, pp. 876–881, Nov. 2015.
- [246] U. Kılıç and K. Ayan, "Optimal power flow solution of two-terminal HVDC systems using genetic algorithm," *Electr. Eng.*, vol. 96, no. 1, pp. 65–77, 2014.
- [247] A. Srujana and S. J. Kumar, "A novel HVDC control strategy to enhance interconnected power systems: A graphicalbased solution," *Amer. J. Sci. Res.*, to be published.
- [248] R. Jackson, O. C. Onar, H. Kirkham, E. Fisher, K. Burkes, M. Starke, O. Mohammed, and G. Weeks, "Opportunities for energy efficiency improvements in the us electricity transmission and distribution system," Oak Ridge Nat. Lab. Oak Ridge U.S. Dept. Energy, Oak Ridge, TN, USA, Tech. Rep., 2015, pp. 3–9.
- [249] M. M. Alharbi, "Modeling of multi-terminal VSC-based HVDC systems," Tech. Rep., 2014.
- [250] Y. Zhou, S. Dalhues, and U. Häger, "Dynamic analysis of voltage angle droop controlled HVDC systems in curative congestion management scenarios," in *Proc. EPJ Web Conf.*, vol. 217, 2019, Art. no. 01004.
- [251] U. Kılıç, K. Ayan, and U. Arifoğlu, "Optimizing reactive power flow of HVDC systems using genetic algorithm," *Int. J. Electr. Power Energy Syst.*, vol. 55, pp. 1–12, Feb. 2014.
- [252] Y. Phulpin, J. Hazra, and D. Ernst, "Model predictive control of HVDC power flow to improve transient stability in power systems," in *Proc. IEEE Int. Conf. Smart Grid Commun. (SmartGridComm)*, Oct. 2011, pp. 593–598.
- [253] R. Wiget and G. Andersson, "Optimal power flow for combined AC and multi-terminal HVDC grids based on VSC converters," in *Proc. IEEE Power Energy Soc. Gen. Meeting*, Jul. 2012, pp. 1–8.
- [254] A. Garces, D. Montoya, and R. Torres, "Optimal power flow in multiterminal HVDC systems considering DC/DC converters," in *Proc. IEEE 25th Int. Symp. Ind. Electron. (ISIE)*, Jun. 2016, pp. 1212–1217.
- [255] A. Venzke and S. Chatzivasileiadis, "Convex relaxations of probabilistic AC optimal power flow for interconnected AC and HVDC grids," *IEEE Trans. Power Syst.*, vol. 34, no. 4, pp. 2706–2718, Jul. 2019.
- [256] S. Bahrami, V. W. S. Wong, and J. Jatskevich, "Optimal power flow for AC–DC networks," in *Proc. IEEE Int. Conf. Smart Grid Commun. (SmartGridComm)*, Nov. 2014, pp. 49–54.

- [257] V. Saplamidis, "Nonlinear security constrained optimal power flow for combined AC and HVDC grids," Ph.D. dissertation, Citeseer, Princeton, NJ, USA, 2014.
- [258] N. Meyer-Huebner, M. Suriyah, and T. Leibfried, "Distributed optimal power flow in hybrid AC-DC grids," *IEEE Trans. Power Syst.*, vol. 34, no. 4, pp. 2937-2946, Jul. 2019.
- [259] V. Saplamidis, R. Wiget, and G. Andersson, "Security constrained optimal power flow for mixed AC and multi-terminal HVDC grids," in *Proc. IEEE Eindhoven PowerTech*, Jun. 2015, pp. 1-6.
- [260] X.-P. Zhang, "Multiterminal voltage-sourced converter-based HVDC models for power flow analysis," *IEEE Trans. Power Syst.*, vol. 19, no. 4, pp. 1877-1884, Nov. 2004.
- [261] M. Nick, R. Cherkaoui, J. L. Boudec, and M. Paolone, "An exact convex formulation of the optimal power flow in radial distribution networks including transverse components," *IEEE Trans. Autom. Control*, vol. 63, no. 3, pp. 682-697, Mar. 2018.
- [262] J. Beerten and R. Belmans, "Development of an open source power flow software for high voltage direct current grids and hybrid AC/DC systems: MATACDC," *IET Gener., Transmiss. Distrib.*, vol. 9, no. 10, pp. 966-974, Jul. 2015.
- [263] A. V. N. Babu and S. Sivanagaraju, "Optimal power flow with FACTS device using two step initialization based algorithm for security enhancement considering credible contingencies," in *Proc. Int. Conf. Adv. Power Convers. Energy Technol. (APCET)*, Aug. 2012, pp. 1-5.
- [264] C. Sourkounis and P. Tourou, "Grid code requirements for wind power integration in Europe," in *Proc. Conf. Papers Energy*. London, U.K.: Hindawi, 2013, pp. 1-11.
- [265] A. Gashi, G. Kabashi, S. Kabashi, S. Ahmetaj, and V. Veliu, "Simulation the wind grid code requirements for wind farms connection in Kosovo transmission grid," Tech. Rep., 2012.
- [266] R. Pinto, S. Rodrigues, E. Wiggelinkhuizen, R. Scherrer, P. Bauer, and J. Pierik, "Operation and power flow control of multi-terminal DC networks for grid integration of offshore wind farms using genetic algorithms," *Energies*, vol. 6, no. 1, pp. 1-26, Dec. 2012.
- [267] W. Qiao and R. G. Harley, "Grid connection requirements and solutions for DFIG wind turbines," in *Proc. IEEE Energy Conf.*, Nov. 2008, pp. 1-8.
- [268] L. Meegahapola, S. Durairaj, D. Flynn, and B. Fox, "Coordinated utilisation of wind farm reactive power capability for system loss optimisation," *Eur. Trans. Electr. Power*, vol. 21, no. 1, pp. 40-51, Jan. 2011.
- [269] V. Rana, R. Gupta, and N. Kumar, "Integration of wind farm into a weak distribution network," *Change*, vol. 5, p. 7, Jan. 2014.
- [270] K. Schönleber, C. Collados, R. T. Pinto, S. Ratés-Palau, and O. Gomis-Bellmunt, "Optimization-based reactive power control in HVDC-connected wind power plants," *Renew. Energy*, vol. 109, pp. 500-509, Aug. 2017.
- [271] I. Erlich, W. Winter, and A. Dittrich, "Advanced grid requirements for the integration of wind turbines into the German transmission system," in *Proc. IEEE Power Eng. Soc. Gen. Meeting*, Jun. 2006, p. 7.
- [272] Z. Chen, "Wind power in modern power systems," *J. Modern Power Syst. Clean Energy*, vol. 1, no. 1, pp. 2-13, Jun. 2013.
- [273] M. N. I. Sarkar, L. G. Meegahapola, and M. Datta, "Reactive power management in renewable rich power grids: A review of grid-codes, renewable generators, support devices, control strategies and optimization algorithms," *IEEE Access*, vol. 6, pp. 41458-41489, 2018.
- [274] S. Kumar, "Reactive power management strategies under distributed generation," Tech. Rep., 2018.
- [275] F. B. Uzunlar, Ö. Guler, and O. Kalenderli, "Grid connection and power quality optimization of wind power plants," in *Proc. 9th Int. Conf. Electr. Electron. Eng. (ELECO)*, Nov. 2015, pp. 415-419.
- [276] P. Yu and B. Venkatesh, "A practical real-time OPF method using new triangular approximate model of wind electric generators," *IEEE Trans. Power Syst.*, vol. 27, no. 4, pp. 2036-2046, Nov. 2012.
- [277] E. Ela, M. Milligan, and B. Kirby, "Operating reserves and variable generation," Nat. Renew. Energy Lab. (NREL), Golden, CO, USA, Tech. Rep., 2011.
- [278] I. Krad, "A reserve-based method for mitigating the impact of renewable energy," Tech. Rep., 2016.
- [279] M. A. Baza and M. Rashidi-Ne, "Dynamical joint energy and spinning reserve dispatch considering transmission network constraint," *J. Appl. Sci.*, vol. 9, no. 7, pp. 1248-1257, Mar. 2009.
- [280] D.-C. Radu, "Strategies for provision of secondary reserve capacity to balance short-term fluctuations of variable renewable energy," Tech. Rep., 2017.
- [281] P. Panagiotakopoulou, "Analysing the effects of future generation and grid investments on the Spanish power market, with large scale wind integration, using Plexos for power systems," Tech. Rep., 2015.
- [282] Q. Wang and B.-M. Hodge, "Enhancing power system operational flexibility with flexible ramping products: A review," *IEEE Trans. Ind. Informat.*, vol. 13, no. 4, pp. 1652-1664, Aug. 2017.
- [283] E. Dall'Anese, K. Baker, and T. Summers, "Optimal power flow for distribution systems under uncertain forecasts," in *Proc. IEEE 55th Conf. Decis. Control (CDC)*, Dec. 2016, pp. 7502-7507.
- [284] H. Zhang and P. Li, "Chance constrained programming for optimal power flow under uncertainty," *IEEE Trans. Power Syst.*, vol. 26, no. 4, pp. 2417-2424, Nov. 2011.
- [285] L. Roald, S. Misra, M. Chertkov, and G. Andersson, "Optimal power flow with weighted chance constraints and general policies for generation control," in *Proc. 54th IEEE Conf. Decis. Control (CDC)*, Dec. 2015, pp. 6927-6933.
- [286] T. Summers, J. Warrington, M. Morari, and J. Lygeros, "Stochastic optimal power flow based on conditional value at risk and distributional robustness," *Int. J. Electr. Power Energy Syst.*, vol. 72, pp. 116-125, Nov. 2015.
- [287] A. Venzke, L. Halilbašić, A. Barré, L. Roald, and S. Chatzivasileiadis, "Chance-constrained AC optimal power flow integrating HVDC lines and controllability," *Int. J. Electr. Power Energy Syst.*, vol. 116, Mar. 2020, Art. no. 105522.
- [288] Z. Wang, C. Shen, F. Liu, X. Wu, C.-C. Liu, and F. Gao, "Chance-constrained economic dispatch with non-Gaussian correlated wind power uncertainty," *IEEE Trans. Power Syst.*, vol. 32, no. 6, pp. 4880-4893, Nov. 2017.
- [289] P. P. Biswas, P. N. Suganthan, and G. A. J. Amaratunga, "Optimal power flow solutions incorporating stochastic wind and solar power," *Energy Convers. Manage.*, vol. 148, pp. 1194-1207, Sep. 2017.
- [290] A. Venzke, L. Halilbasic, U. Markovic, G. Hug, and S. Chatzivasileiadis, "Convex relaxations of chance constrained AC optimal power flow," *IEEE Trans. Power Syst.*, vol. 33, no. 3, pp. 2829-2841, May 2018.
- [291] M. Lubin, Y. Dvorkin, and L. Roald, "Chance constraints for improving the security of AC optimal power flow," *IEEE Trans. Power Syst.*, vol. 34, no. 3, pp. 1908-1917, May 2019.
- [292] W. Xie and S. Ahmed, "Distributionally robust chance constrained optimal power flow with renewables: A conic reformulation," *IEEE Trans. Power Syst.*, vol. 33, no. 2, pp. 1860-1867, Mar. 2018.
- [293] O. D. Montoya and W. Gil-González, "On the numerical analysis based on successive approximations for power flow problems in AC distribution systems," *Electric Power Syst. Res.*, vol. 187, Oct. 2020, Art. no. 106454.
- [294] A. Chanhome and S. Chaitusaney, "Development of three-phase unbalanced power flow using local control of connected photovoltaic systems," *IEEJ Trans. Electr. Electron. Eng.*, vol. 15, no. 6, pp. 833-843, Jun. 2020.
- [295] J.-H. Menke, N. Bornhorst, and M. Braun, "Distribution system monitoring for smart power grids with distributed generation using artificial neural networks," *Int. J. Electr. Power Energy Syst.*, vol. 113, pp. 472-480, Dec. 2019.
- [296] A. Di Fazio, M. Russo, and M. D. Santis, "Zoning evaluation for voltage optimization in distribution networks with distributed energy resources," *Energies*, vol. 12, no. 3, p. 390, Jan. 2019.
- [297] E. Dall'Anese and A. Simonetto, "Optimal power flow pursuit," *IEEE Trans. Smart Grid*, vol. 9, no. 2, pp. 942-952, Mar. 2018.
- [298] Y. Zhang, M. Hong, E. Dall'Anese, S. V. Dhople, and Z. Xu, "Distributed controllers seeking AC optimal power flow solutions using ADMM," *IEEE Trans. Smart Grid*, vol. 9, no. 5, pp. 4525-4537, Sep. 2018.
- [299] Z. Zhu, D. Liu, Q. Liao, F. Tang, J. Zhang, and H. Jiang, "Optimal power scheduling for a medium voltage AC/DC hybrid distribution network," *Sustainability*, vol. 10, no. 2, p. 318, Jan. 2018.
- [300] S. A. F. Asl, L. Bagherzadeh, S. Pirouzi, M. Norouzi, and M. Lehtonen, "A new two-layer model for energy management in the smart distribution network containing flexi-renewable virtual power plant," *Electr. Power Syst. Res.*, vol. 194, May 2021, Art. no. 107085.
- [301] Q. Peng, Z. Yuan, B. Ouyang, P. Guo, and L. Qu, "Research on the optimal operation method of DC microgrid base on the new DC power distribution management system," *Electronics*, vol. 9, no. 1, p. 9, Dec. 2019.

- [302] Y. Chen, W. Wei, F. Liu, E. E. Sauma, and S. Mei, "Energy trading and market equilibrium in integrated heat-power distribution systems," *IEEE Trans. Smart Grid*, vol. 10, no. 4, pp. 4080–4094, Jul. 2019.
- [303] T. Soares and R. J. Bessa, "Proactive management of distribution grids with chance-constrained linearized AC OPF," *Int. J. Electr. Power Energy Syst.*, vol. 109, pp. 332–342, Jul. 2019.
- [304] M. Vahedipour-Dahraie, H. Rashidzadeh-Kermani, A. Anvari-Moghaddam, and J. M. Guerrero, "Stochastic risk-constrained scheduling of renewable-powered autonomous microgrids with demand response actions: Reliability and economic implications," *IEEE Trans. Ind. Appl.*, vol. 56, no. 2, pp. 1882–1895, Mar. 2020.
- [305] H. Haghighat, H. Karimianfard, and B. Zeng, "Integrating energy management of autonomous smart grids in electricity market operation," *IEEE Trans. Smart Grid*, vol. 11, no. 5, pp. 4044–4055, Sep. 2020.
- [306] M. A. Mirzaei, M. Hemmati, K. Zare, M. Abapour, B. Mohammadi-Ivatloo, M. Marzband, and A. Anvari-Moghaddam, "A novel hybrid two-stage framework for flexible bidding strategy of reconfigurable micro-grid in day-ahead and real-time markets," *Int. J. Electr. Power Energy Syst.*, vol. 123, Dec. 2020, Art. no. 106293.
- [307] B. Wei, S. Claeys, H. Almasalma, and G. Deconinck, "Stochastic distributed optimization of shapeable energy resources in low voltage distribution networks under limited communications," *Int. J. Energy Res.*, vol. 45, no. 1, pp. 991–1006, Jan. 2021.
- [308] E. Dall'Anese, K. Baker, and T. Summers, "Chance-constrained AC optimal power flow for distribution systems with renewables," *IEEE Trans. Power Syst.*, vol. 32, no. 5, pp. 3427–3438, Sep. 2017.
- [309] S. Park and S. R. Salkuti, "Optimal energy management of railroad electrical systems with renewable energy and energy storage systems," *Sustainability*, vol. 11, no. 22, p. 6293, Nov. 2019.
- [310] Y. Fu, Z. Zhang, Z. Li, and Y. Mi, "Energy management for hybrid AC/DC distribution system with microgrid clusters using non-cooperative game theory and robust optimization," *IEEE Trans. Smart Grid*, vol. 11, no. 2, pp. 1510–1525, Mar. 2020.
- [311] O. D. Montoya, F. M. Serra, and C. H. De Angelo, "On the efficiency in electrical networks with AC and DC operation technologies: A comparative study at the distribution stage," *Electronics*, vol. 9, no. 9, p. 1352, Aug. 2020.
- [312] J. F. Franco, L. F. Ochoa, and R. Romero, "AC OPF for smart distribution networks: An efficient and robust quadratic approach," *IEEE Trans. Smart Grid*, vol. 9, no. 5, pp. 4613–4623, Sep. 2018.
- [313] S. Duman, J. Li, L. Wu, and N. Yorukeren, "Symbiotic organisms search algorithm-based security-constrained AC–DC OPF regarding uncertainty of wind, PV and PEV systems," *Soft Comput.*, vol. 25, no. 14, pp. 9389–9426, Jul. 2021.
- [314] N. Chowdhury, F. Pilo, and G. Pisano, "Optimal energy storage system positioning and sizing with robust optimization," *Energies*, vol. 13, no. 3, p. 512, Jan. 2020.
- [315] M. Giuntoli, M. Subasic, and S. Schmitt, "Control of distribution grids with storage using nested Benders' decomposition," *Electr. Power Syst. Res.*, vol. 190, Jan. 2021, Art. no. 106663.
- [316] M. Dabbaghjamesh, A. Kavousi-Fard, S. Mehraeen, J. Zhang, and Z. Y. Dong, "Sensitivity analysis of renewable energy integration on stochastic energy management of automated reconfigurable hybrid AC–DC microgrid considering DLR security constraint," *IEEE Trans. Ind. Informat.*, vol. 16, no. 1, pp. 120–131, Jan. 2020.
- [317] F. Molina-Martin, O. D. Montoya, L. F. Grisales-Noreña, J. C. Hernández, and C. A. Ramírez-Vanegas, "Simultaneous minimization of energy losses and greenhouse gas emissions in AC distribution networks using BESS," *Electronics*, vol. 10, no. 9, p. 1002, Apr. 2021.
- [318] B. Morvaj, R. Evins, and J. Carmeliet, "Decarbonizing the electricity grid: The impact on urban energy systems, distribution grids and district heating potential," *Appl. Energy*, vol. 191, pp. 125–140, Apr. 2017.
- [319] A. Saint-Pierre and P. Mancarella, "Active distribution system management: A dual-horizon scheduling framework for DSO/TSO interface under uncertainty," *IEEE Trans. Smart Grid*, vol. 8, no. 5, pp. 2186–2197, Sep. 2017.
- [320] E. Grover-Silva, R. Girard, and G. Kariniotakis, "Optimal sizing and placement of distribution grid connected battery systems through an SOCP optimal power flow algorithm," *Appl. Energy*, vol. 219, pp. 385–393, Jun. 2018.
- [321] N. Nazir, P. Racherla, and M. Almassalkhi, "Optimal multi-period dispatch of distributed energy resources in unbalanced distribution feeders," *IEEE Trans. Power Syst.*, vol. 35, no. 4, pp. 2683–2692, Jul. 2020.
- [322] H. Saber, H. Mazaheri, H. Ranjbar, M. Moeini-Aghtaie, and M. Lehtonen, "Utilization of in-pipe hydropower renewable energy technology and energy storage systems in mountainous distribution networks," *Renew. Energy*, vol. 172, pp. 789–801, Jul. 2021.
- [323] T. Liu, X. Tan, B. Sun, Y. Wu, and D. H. K. Tsang, "Energy management of cooperative microgrids: A distributed optimization approach," *Int. J. Electr. Power Energy Syst.*, vol. 96, pp. 335–346, Mar. 2018.
- [324] V. Grimm, J. Grübel, B. Rückel, C. Sölch, and G. Zöttl, "Storage investment and network expansion in distribution networks: The impact of regulatory frameworks," *Appl. Energy*, vol. 262, Mar. 2020, Art. no. 114017.
- [325] I. Naidji, M. Ben Smida, M. Khalgui, A. Bachir, Z. Li, and N. Wu, "Efficient allocation strategy of energy storage systems in power grids considering contingencies," *IEEE Access*, vol. 7, pp. 186378–186392, 2019.
- [326] Q. Gemine, D. Ernst, and B. Cornélusse, "Active network management for electrical distribution systems: Problem formulation, benchmark, and approximate solution," *Optim. Eng.*, vol. 18, no. 3, pp. 587–629, Sep. 2017.
- [327] S. Zhou, Y. Zhao, W. Gu, Z. Wu, Y. Li, Z. Qian, and Y. Ji, "Robust energy management in active distribution systems considering temporal and spatial correlation," *IEEE Access*, vol. 7, pp. 153635–153649, 2019.
- [328] S. A. Bozorgavari, J. Aghaei, S. Pirouzi, V. Vahidinasab, H. Farahmand, and M. Korpás, "Two-stage hybrid stochastic/robust optimal coordination of distributed battery storage planning and flexible energy management in smart distribution network," *J. Energy Storage*, vol. 26, Dec. 2019, Art. no. 100970.
- [329] B. Morvaj, K. Knezović, R. Evins, and M. Marinelli, "Integrating multi-domain distributed energy systems with electric vehicle PQ flexibility: Optimal design and operation scheduling for sustainable low-voltage distribution grids," *Sustain. Energy, Grids Netw.*, vol. 8, pp. 51–61, Dec. 2016.
- [330] R. Hemmati, S. M. S. Ghiasi, and A. Entezariharsini, "Power fluctuation smoothing and loss reduction in grid integrated with thermal-wind-solar-storage units," *Energy*, vol. 152, pp. 759–769, Jun. 2018.
- [331] H. Xiao, W. Pei, W. Deng, T. Ma, S. Zhang, and L. Kong, "Enhancing risk control ability of distribution network for improved renewable energy integration through flexible DC interconnection," *Appl. Energy*, vol. 284, Feb. 2021, Art. no. 116387.
- [332] S. Nowak, L. Wang, and M. S. Metcalfe, "Two-level centralized and local voltage control in distribution systems mitigating effects of highly intermittent renewable generation," *Int. J. Electr. Power Energy Syst.*, vol. 119, Jul. 2020, Art. no. 105858.
- [333] L. Zhang, Y. Chen, C. Shen, W. Tang, J. Liang, and B. Xu, "Optimal configuration of hybrid AC/DC urban distribution networks for high penetration renewable energy," *IET Gener., Transmiss. Distrib.*, vol. 12, no. 20, pp. 4499–4506, Nov. 2018.
- [334] W. Wei, Z. Shen, L. Wu, F. Li, and T. Ding, "Estimating DLMP confidence intervals in distribution networks with AC power flow model and uncertain renewable generation," *IET Gener., Transmiss. Distrib.*, vol. 14, no. 8, pp. 1467–1475, Apr. 2020.
- [335] H. M. A. Ahmed, A. B. Eltantawy, and M. M. A. Salama, "A planning approach for the network configuration of AC-DC hybrid distribution systems," *IEEE Trans. Smart Grid*, vol. 9, no. 3, pp. 2203–2213, May 2018.
- [336] L. Yao, X. Wang, Y. Li, C. Duan, and X. Wu, "Distributionally robust chance-constrained AC-OPF for integrating wind energy through multi-terminal VSC-HVDC," *IEEE Trans. Sustain. Energy*, vol. 11, no. 3, pp. 1414–1426, Jul. 2020.
- [337] R. Mieth and Y. Dvorkin, "Distribution electricity pricing under uncertainty," *IEEE Trans. Power Syst.*, vol. 35, no. 3, pp. 2325–2338, May 2020.
- [338] M. Akbari, J. Aghaei, and M. Barani, "Convex probabilistic allocation of wind generation in smart distribution networks," *IET Renew. Power Gener.*, vol. 11, no. 9, pp. 1211–1218, Jul. 2017.
- [339] S. Rezaeian-Marjani, S. Galvani, V. Talavat, and M. Farhadi-Kangarlu, "Optimal allocation of D-STATCOM in distribution networks including correlated renewable energy sources," *Int. J. Electr. Power Energy Syst.*, vol. 122, Nov. 2020, Art. no. 106178.

- [340] D. A. Quijano and A. Padilha-Feltrin, "Optimal integration of distributed generation and conservation voltage reduction in active distribution networks," *Int. J. Electr. Power Energy Syst.*, vol. 113, pp. 197–207, Dec. 2019.
- [341] Y. Xu, M. Korkali, L. Mili, J. Valinejad, T. Chen, and X. Chen, "An iterative response-surface-based approach for chance-constrained AC optimal power flow considering dependent uncertainty," *IEEE Trans. Smart Grid*, vol. 12, no. 3, pp. 2696–2707, May 2021.
- [342] Y. Sang, M. Sahraei-Ardakani, and M. Parvania, "Stochastic transmission impedance control for enhanced wind energy integration," *IEEE Trans. Sustain. Energy*, vol. 9, no. 3, pp. 1108–1117, Jul. 2018.
- [343] S. Magnússon, G. Qu, and N. Li, "Distributed optimal voltage control with asynchronous and delayed communication," *IEEE Trans. Smart Grid*, vol. 11, no. 4, pp. 3469–3482, Jul. 2020.
- [344] A. S. Zamzam, N. D. Sidiropoulos, and E. Dall'Anese, "Beyond relaxation and Newton–Raphson: Solving AC OPF for multi-phase systems with renewables," *IEEE Trans. Smart Grid*, vol. 9, no. 5, pp. 3966–3975, Sep. 2018.
- [345] H. M. A. Ahmed and M. M. A. Salama, "Energy management of AC–DC hybrid distribution systems considering network reconfiguration," *IEEE Trans. Power Syst.*, vol. 34, no. 6, pp. 4583–4594, Nov. 2019.
- [346] M. A. El-salam, E. Beshr, and M. Eteiba, "A new hybrid technique for minimizing power losses in a distribution system by optimal sizing and siting of distributed generators with network reconfiguration," *Energies*, vol. 11, no. 12, p. 3351, Nov. 2018.
- [347] C. Duan, W. Fang, L. Jiang, L. Yao, and J. Liu, "Distributionally robust chance-constrained approximate AC-OPF with Wasserstein metric," *IEEE Trans. Power Syst.*, vol. 33, no. 5, pp. 4924–4936, Sep. 2018.
- [348] F. Sun, J. Ma, M. Yu, and W. Wei, "A robust optimal coordinated droop control method for multiple VSCs in AC–DC distribution network," *IEEE Trans. Power Syst.*, vol. 34, no. 6, pp. 5002–5011, Nov. 2019.
- [349] M. Z. Liu, L. F. Ochoa, and S. H. Low, "On the implementation of OPF-based setpoints for active distribution networks," *IEEE Trans. Smart Grid*, vol. 12, no. 4, pp. 2929–2940, Jul. 2021.
- [350] T. Abreu, T. Soares, L. Carvalho, H. Morais, T. Simao, and M. Louro, "Reactive power management considering stochastic optimization under the Portuguese reactive power policy applied to DER in distribution networks," *Energies*, vol. 12, no. 21, p. 4028, Oct. 2019.
- [351] W. Sun, S. Harrison, and G. P. Harrison, "Value of local offshore renewable resource diversity for network hosting capacity," *Energies*, vol. 13, no. 22, p. 5913, Nov. 2020.



**ZONGJIE WANG** (Member, IEEE) is currently an Assistant Professor with the Department of Electrical and Computer Engineering, University of Connecticut (UConn). She is also affiliated with the Eversource Energy Center. Prior to joining UConn, she was a Postdoctoral Research Associate in systems engineering with Cornell University. Her research interests include modern power systems, grid resilience, renewable energy integration through leveraging data analytics, non-linear optimization, and simulation techniques. Her research has been funded by the U.S. Department of Energy, Eversource Energy, and UConn OVPR.



**ABDOLLAH YOUNESI** (Member, IEEE) received the B.Sc., M.Sc., and Ph.D. degrees in electrical engineering from the Faculty of Technical Engineering, Mohaghegh Ardabili University, Ardabil, Iran, in 2012, 2015, and 2021, respectively. He was a Senior Research Associate with the School of Computing Science, University of East Anglia, Norwich, U.K., in 2022. He is currently a Researcher with the Department of Electrical Engineering, University of Connecticut, CT, USA. Throughout his academic career, he has been selected as a talent student of the university several times in B.Sc., M.Sc., and Ph.D. degrees. In addition, he was chosen as the top talent of the National Elite Foundation of Iran twice, in 2018 and 2019. His research interests include mini/micro-grids, resilient operation of power systems, power system dynamics, game theory, power system stability, control, application of artificial intelligence in power, and renewable and storage energy resources.



**M. VIVIENNE LIU** (Student Member, IEEE) received the bachelor's degree in electrical and information engineering from Tianjin University and the master's degree in electrical engineering from Stanford University. She is currently pursuing the Ph.D. degree in systems engineering. Her research interest includes control and optimization of smart grids with renewable energy integration. Her current research interest includes using multi-objective simulation-based optimization methods to help inform policies on the management of microgrids energy systems.



**GE CLAIRE GUO** (Member, IEEE) received the M.S. degree in industrial engineering from Texas A&M University and the Ph.D. degree in industrial engineering from Iowa State University. She is currently an Assistant Professor in operations research with the Merrick School of Business, University of Baltimore. Her expertise lies in stochastic integer optimization with applications on renewable power systems. Prior to joining the University of Baltimore, she was a Postdoctoral Associate in systems engineering with Cornell University.



**C. LINDSAY ANDERSON** (Senior Member, IEEE) is currently a Professor and the Chair of Biological and Environmental Engineering with Cornell University and the Interim Director of the Cornell Energy Systems Institute. She teaches and conducts research in the areas of sustainable energy and the environment, with a particular focus on the integration of renewable and distributed resources in electric power grid operations. Her research has been funded by the U.S. National Science Foundation, the Natural Sciences and Engineering Research Council of Canada, the U.S. Department of Energy, and the Cornell Atkinson Center for Sustainability.

...